RESEARCH ARTICLE

FractalSpiNet: Fractal-Based U-Net for Automatic Segmentation of Cervical Spinal Cord and MS Lesions in MRI

RUKİYE POLATTİMUR[ID][1], **EMRE DANDIL**[ID][2], **MEHMET SÜLEYMAN YILDIRIM**[ID][3], **SÜLEYMAN ULUÇAY**[4], **AND UTKU ŞENOL**[4]

[1]Department of Electronics and Computer Engineering, Institute of Graduate, Bilecik Şeyh Edebali University, 11230 Bilecik, Türkiye
[2]Department of Computer Engineering, Faculty of Engineering, Bilecik Şeyh Edebali University, 11230 Bilecik, Türkiye
[3]Department of Computer Technologies, Sogut Vocational School, Bilecik Şeyh Edebali University, 11230 Bilecik, Türkiye
[4]Department of Radiology, Faculty of Medicine, Akdeniz University, 07070 Antalya, Türkiye

Corresponding author: Emre Dandil (emre.dandil@bilecik.edu.tr)

ABSTRACT The spinal cord is an important part of the central nervous system, responsible for transmitting nerve signals throughout the body. The cervical spinal cord contains eight nerve bundles located in the neck region of the spinal cord that transmit to the face and head region. For this reason, in addition to traditional methods of monitoring changes in the spinal cord region in routine clinical practice, spinal cord segmentation using innovative computer-based systems makes an important contribution to the understanding of disease progression. Lesions in the cervical spinal cord can be a symptom of several neurological diseases, especially demyelinating diseases such as multiple sclerosis (MS). The detection of lesions in the spinal cord is particularly important in diseases such as MS, which affect a wide age range and for which early diagnosis is crucial. Therefore, automated segmentation of the spinal cord to quantify spinal cord atrophy is critical for changes in the human spinal cord. In addition to clinical findings, magnetic resonance imaging (MRI) technologies have improved the quality of images for monitoring, diagnosing and determining the treatment protocol for MS lesions in the spinal cord. However, due to the difficulty of scanning the cervical spinal cord region and the occurrence of artefacts during acquisition, it is very difficult to determine the spinal cord boundaries and detect lesions in this region. In this study, we propose a fractal network-based U-Net (FractalSpiNet) deep learning architecture for automatic segmentation of the spinal cord and spinal cord MS lesions from cervical spinal cord MR slices. The developed FractalSpiNet architecture incorporate a fractal network for enhanced feature extraction in MRI scans. In addition, a new dataset of axial plane MR images from the cervical spinal cord of 87 MS patients is first created in the study. Using the proposed FractalSpiNet architecture, the cross-sectional area of the cervical spinal cord was segmented with a Dice Similarity Coefficient (DSC) score of 98.88%, while MS lesions in the cervical spinal cord were detected with a DSC score of 90.90%. These results indicate that FractalSpiNet provides results that close to expert mask for segmentation of cervical spinal cord and MS lesion detection. The experimental studies also compare the results of the proposed FractalSpiNet with the results of state-of-the-art hybrid U-Net models such as base U-Net, Attention U-Net, Residual U-Net, and Attention Residual U-Net. In conclusion, the experimental results demonstrate the effectiveness of our approach in achieving accurate segmentation of cervical spinal cord and MS lesions, outperforming state-of-the-art methods. The proposed FractalSpiNet offers a promising

The associate editor coordinating the review of this manuscript and approving it for publication was Prakasam Periasamy[ID].

approach for automated segmentation of the cervical spinal cord and MS lesions, potentially aiding in the diagnosis and treatment of neurological disorders.

INDEX TERMS Cervical spinal cord, multiple sclerosis, automatic segmentation, fractal networks, U-Net, FractalSpiNet.

I. INTRODUCTION

The spinal cord is part of the central nervous system and its anatomical structure is very complex, as it is part of the spinal canal [1]. The cervical spinal cord is a segment of the spinal cord located in the neck of the spine and forms the transition zone for many important functional pathways in the body. The cervical spinal cord - the neck of the spine - consists of seven stacked vertebrae from C1 to C7. The cervical spinal cord runs through the centre of the cervical spine [2]. The cervical spinal cord, as the centre through which motor and sensory nerves flow, controls arm and shoulder movements and transmits sensory information from the body to the brain [3]. Accurate segmentation of the cervical spinal cord is therefore a critical step in the diagnosis and treatment of neurological disorders.

The cervical spinal cord is the transit zone for many important tracts and nerve roots that affect the upper part of the body, such as the arm and shoulder. These tracts provide communication between the brain and the body and regulate movement, sensation and other neural functions. The cervical spinal cord is also a region affected by many neurological disorders. Various conditions such as spinal cord injury, degenerative diseases such as multiple sclerosis (MS), infections and tumours can affect the cervical spinal cord [4]. Therefore, accurate anatomical and functional assessment and imaging of the cervical spinal cord is important in the diagnosis and treatment of neurological disorders. Magnetic resonance imaging (MRI) is therefore widely used in the examination and follow-up of the cervical spinal cord.

The cervical spinal cord is a common area of MS lesions. MS is a chronic, demyelinating, neurodegenerative autoimmune disease that affects the central nervous system (CNS) [5], [6]. It is characterised by damage and inflammation of the myelin sheath that surrounds the brain and spinal cord. MS is an inflammatory disease of the central nervous system, often affecting structures such as the brain and spinal cord. MS affects the brain, spinal cord and optic nerves and is caused by the accumulation of demyelinating plaques in the white and grey matter. A wealth of epidemiological data has been obtained from studies of MS conducted over a long period of time. However, it is still a difficult task to model the geographical distribution of MS worldwide [7]. According to the World Health Organisation, more than 1.8 million people worldwide have MS, and although it affects people of all ages, it is more common in young adults and especially in women [8].

Although MS lesions can be seen along the entire spinal cord, including the cervical, thoracic and lumbar regions, they are most commonly seen in the cervical spinal cord and MS lesions are usually looked for in this region on MR scans [9], [10]. Clinical follow-up of the cervical spinal cord and MS lesions in this region, and treatment planning based on MR findings, are possible thanks to the rapid development of MR technology. However, structural differences, regional difficulties or pathological reasons in the area of the spinal cord being imaged can affect the quality of the medical imaging and lead to suboptimal performance [11], [12]. On conventional spine sequences, spinal cord lesions are visualized as areas of T2 hyperintensity and less commonly as areas of T1 hypointensity [13]. MS lesions occur most frequently (59%) in the cervical spinal cord and less frequently (20%) in the lower thoracic spinal cord (T7-12) [14]. In contrast, MS lesions often appear cylindrical on sagittal MR images and wedge-shaped on axial MR images, and typically have sharp borders [15]. In sagittal views, their length rarely exceeds two vertebral segments. On axial scans, MS lesions occupy less than 50% of the slice area, preferentially occupying the lateral and posterior white matter columns and not sparing the grey matter. Recommended protocols for spinal cord MRI in the clinical setting include both sagittal and axial MR scans [16].

Accurate segmentation of the cervical spinal cord and detection of MS lesions allows early and accurate diagnosis of disease [17]. Traditionally, manual assessment methods based on expert observation have been used to detect and evaluate cervical spinal cord and MS lesions. However, these methods can be subjective and time-consuming, and may also be limited in their ability to accurately detect the number, size and distribution of lesions. Therefore, automated segmentation methods have significant potential for accurate and reliable identification of MS lesions in MR images of the cervical spinal cord. Automatic segmentation methods can process large datasets quickly, saving time and reducing subjective errors. In recent years, deep learning techniques and artificial intelligence have led to significant advances in automatic segmentation of the spinal cord.

While advancements in MRI technology have improved image quality, challenges like image artifacts due to motion or scanner imperfections can hinder accurate and consistent segmentation, especially in the complex cervical region. Existing automated segmentation methods might not capture the full complexity of the cervical spinal cord and MS lesions, particularly in cases with subtle lesions or challenging image quality. This can lead to missed diagnoses or inaccurate treatment plans. Therefore, there is a critical need for a robust and fully automatic segmentation method that can overcome these limitations and achieve accurate segmentation of the

cervical spinal cord and MS lesions in MR scans, even in the presence of image artifacts. To the best of our knowledge, the number of previously proposed works that provide fully automatic segmentation of the cervical spinal cord from MR scans and detection of MS lesions therein is very limited. To fill this gap, in this work, we propose the FractalSpiNet architecture, a fully automatic fractal network-based U-Net model for cervical spinal cord segmentation and MS lesion detection. The FractalSpiNet framework is designed to start with a new dataset obtained from the study, first locate the cervical spinal cord, then localise the cervical spinal cord region and perform segmentation. The final step is to detect MS lesions in the cervical spinal cord region. The key novelty of FractalSpiNet lies in its ability to apply fractal convolution instead of regular convolution to U-Net architecture using multi-scale processing.

The contributions of the proposed FractalSpiNet architecture to the segmentation of the cervical spinal cord region and the detection of MS lesions within these boundaries:

1- Preparation of a new dataset of MR scans for the cervical spinal cord
2- Fully automatic segmentation of the cervical spinal cord using the proposed FractalSpiNet architecture
3- Successful detection of MS lesions in the cervical spinal cord region with the proposed FractalSpiNet architecture
4- Comparison of the performance of the proposed FractalSpiNet architecture with state-of-the-art methods using key metrics
5- Designing an assistant framework that experts can use in the decision-making process for the detection of cervical spinal cord and MS lesions on MR scans
6- FractalSpiNet represents a significant advancement in the field of cervical spinal cord segmentation, offering a reliable and efficient solution that is adaptable to various clinical scenarios, thereby improving diagnostic accuracy and patient outcomes, particularly MS.

The rest of the study are organised as follows: Section II reviews related work in the field of cervical spinal cord segmentation and MS lesion detection. Section III presents the details of the prepared original dataset, image pre-processing steps and the proposed FractalSpiNet architecture in detail. Section IV explains the parameters used in the architecture and the results obtained for experimental analyses as a result of model training. In addition, this section compares the performance of FractalSpiNet with other state-of-the-art methods. Section V discusses the implications of the findings and compares the results obtained by the proposed FractalSpiNet model with other previously proposed methods and discusses the results. The last section concludes the paper with a summary of the contributions and key results.

II. RELATED WORKS
Innovative approaches are often used to overcome traditional clinical challenges in cervical spinal cord segmentation and

MS lesion detection. In this context, many contributions have been made in recent years to the detection and automatic segmentation of the spinal cord region of interest and lesion areas using MR images. Using various MR planes such as axial, coronal and sagittal, and different acquisition modalities such as T1-weighted (T1-w) and T2-weighted (T2-w) with manual or automated models, different approaches to spinal cord segmentation and lesion detection have been presented from the past to the present [17]. Different segmentation techniques are proposed for the spinal cord region, white matter (WM), grey matter (GM), cross-sectional area (CSA) and for the detection of different spinal cord lesions.

Manual [18], semi-automatic [19], [20] and fully automatic [21], [22], [23], [24], [25], [26] methods have been proposed for spinal cord segmentation using different techniques and approaches. More recently, deep learning-based approaches have also been proposed for spinal cord detection [27], [28], [29]. However, the number of studies proposed for spinal cord segmentation and MS lesion detection is limited. In a proposed semi-automated study, El Mendili et al. [20] proposed a semi-automated double-threshold based method for segmentation of the cervical and thoracic spinal cord from T2-w MR images. They analysed MR scans from healthy subjects, patients with amyotrophic lateral sclerosis, spinal muscular atrophy and spinal cord injury. They also evaluated the results obtained by comparing the proposed semi-automatic method with the active surface method and the threshold-based method.

Cadotte et al. [30] proposed a semi-automatic algorithm to find the centreline of the human cervical spinal cord and measure the distances from a fixed point in the brainstem to each of the spinal roots and vertebral bodies.

Gros et al. [24] proposed the structure of the OptiC algorithm, which attempts to strike a balance between the probabilistic localisation map of the spinal cord midpoint in the cervical spinal cord and the overall spatial coherence of the spinal cord midline using MR images of patients with neurological disorders from different centres. In order to obtain more consistent boundaries, a process is added that separates the spinal cord centre line from the boundaries of the brain regions. When comparing the proposed OptiC with the spinal cord localisation technique based on the Hough transform, it is highlighted that successful results are obtained in pathological cases.

Deep learning methods are much more advantageous in terms of time and cost. This is because the best feature sets that characterise the data are created to solve problems related to machine learning, whereas in deep learning this approach has been replaced by creating an architecture to automate feature processing. In a fully automated study on spinal cord localisation, Gros et al. [31] presented two sequential CNN approaches for segmentation of cervical spinal cord and MS lesions from MR scans. In addition, the study provided segmentation of the spinal cord and lesion, including detection of the spinal cord midline. The results of the study are also compared with another state-of-the-art method. In addition,

the proposed approach was developed into an open-source framework. In the study, the spinal cord segmentation results of the proposed method outperformed the existing studies, but remained close to the manual segmentation results in MS lesion detection.

In another study, McCoy et al. [32] detected the cervical spinal cord region and intramedullary spinal cord lesions from the full axial plane using their proposed 2D CNN-based image analysis pipeline. In the method, a dataset of MR images obtained from patients with spinal cord injury within 24 hours was generated. Although the 2D CNN architectures developed in the study were compared, it was found that the proposed models did not differ significantly in terms of performance.

In their own study, Merali et al. [28] developed a deep learning-based model using ResNet-50 architecture to identify cervical spinal cord compression in patients with degenerative cervical myelopathy from T2-w MR images. However, they emphasised that for the proposed model to perform better, data has to be acquired only from patients with degenerative cervical myelopathy (DCM), and asymptomatic patients or patients with mild DCM symptoms should be included in model training, resulting in more diverse training images and perhaps a more generalisable model. In addition, the manual ground truth generation process performed by the expert was also identified as a limitation.

The U-Net architecture performs the extraction of the specific region to be segmented on the images and shows more successful performance with less data compared to other deep learning models with advanced feature selection. In particular, in medical image processing, spinal cord region segmentation using MR images scanned from different planes [33], [34], automatic segmentation and classification of spinal cord tumours and lesions [35], [36], [37] are also performed using U-Net models, which provide stable and powerful results in many aspects. Zhang et al. [38] proposed a channel-attentive U-net model for segmentation of the cervical spinal cord from MR scans. In the study, a new dataset of cervical spinal cord MR scans was generated. The proposed model adds double convolution for feature extraction. The results obtained in the study were compared with other previously proposed state-of-the-art methods and the results were found to be close to each other.

Based on the provided previous works, although many studies have been proposed, they have some limitations and there are still parts that need to be improved.

i. Overall, research in this area is limited compared to other medical image segmentation tasks.

ii. Many studies suffer from the use of small datasets, which can lead to overfitting and limit the model's generalizability to unseen data. Additionally, some studies lack diversity in the data, focusing on specific patient populations.

iii. Traditional methods rely on manual feature extraction, which can be time-consuming, subjective, and require expert knowledge.

iv. Studies comparing proposed methods with existing ones often show similar performance, suggesting a need for significant advancements in segmentation accuracy, especially for MS lesion detection.

v. Some studies focus solely on cervical spinal cord segmentation or MS lesion detection, neglecting the potential for a combined approach.

These limitations highlight the need for further research in automatic segmentation of cervical spinal cord and detection of MS lesions, focusing on larger and more diverse datasets, improved deep learning architectures, and standardized evaluation metrics. Additionally, exploring combined approaches for segmentation and lesion detection within a single framework could be beneficial.

This study proposes a new model, FractalSpiNet, for automatic segmentation of the cervical spinal cord and automatic detection of MS lesions in this region. In this model, a new hybrid model is developed by integrating the convolutional structure of FractalSpiNet into the U-Net architecture. In this study, the cervical spinal cord region is segmented using axial plane MR images and MS lesions are detected using the proposed model.

III. MATERIALS AND METHODS

In this study, automatic detection of the cervical spinal cord region and MS lesions in this region was performed using the proposed FractalSpiNet with a new dataset created from axial-plane T2-w MR slices. The methodology of the proposed FractalSpiNet model is shown in Fig. 1. In the study, an original dataset was first created using MR scans from Akdeniz University Hospital. Fig. 1 (a) shows a series of MR scans in the original dataset and the ground truth masks prepared for each MR slice. Then, in Fig. 1 (b), image pre-processing procedures such as resampling and cropping were applied to the MR slices, followed by data enhancement. Here, the pre-processing is included and represents the 320×250 MR slices and the cropping process applied to the masks resulting in 128×128 images. For the next step, Fig. 1 (c) represents the augmented dataset obtained using data augmentation techniques using the cropped images. In Fig 1 (d), the dataset, divided into training and test sets, was trained with the proposed FractalSpiNet network to obtain the optimal weights. In the last step, using FractalSpiNet in Fig 1. (e), the predictive ability of the proposed FractalSpiNet model for cervical spinal cord segmentation and MS lesions is analysed. MS lesions, CSA region and non-MS CSA region are detected from axial spinal cord images in the test set using FractalSpiNet.

A. DATASET

The cervical region is located approximately at the level of the C1-C7 intervertebral disc of the spinal cord. In this study, with the decision of the Clinical Research Ethics Committee of the Faculty of Medicine of Akdeniz University dated 15.09.2021 and numbered KAEK-644, a new dataset was
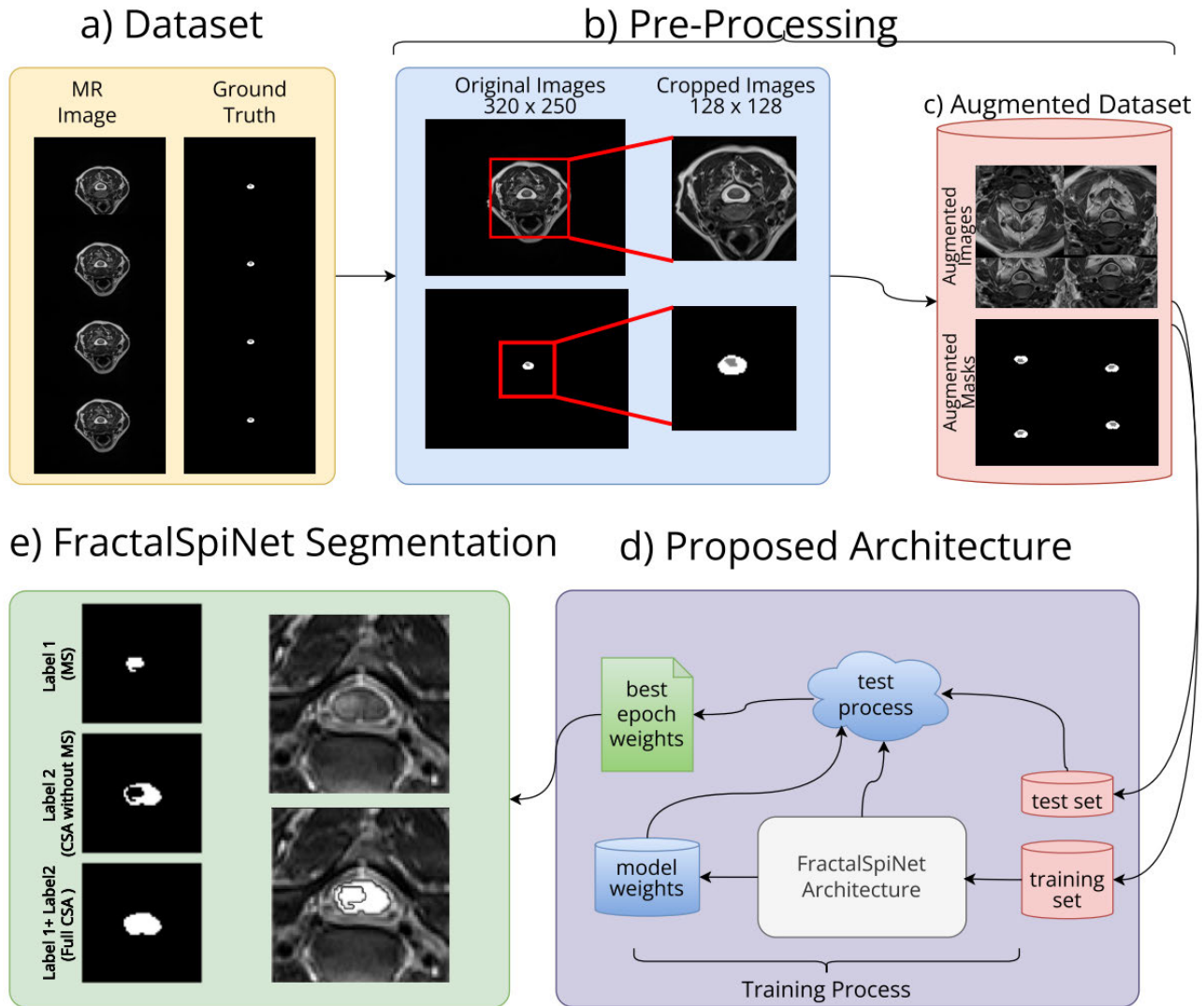
FIGURE 1. The methodology of the proposed FractalSpiNet architecture for automatic segmentation of the cervical spinal cord and MS lesions from axial planes. (a) A set of original MR scans and ground truth masks prepared for each MR slice, (b) includes pre-processing and refers to the 320 × 250 MR slices and the images obtained in 128 × 128 size as a result of the cropping process applied to the masks, (c) refers to the augmented dataset obtained by data augmentation techniques using the cropped images, (d) separating the data set into 20% test set and 80% training set and obtaining the results with the best epoch value obtained as a result of training the proposed FractalSpiNet model, (e) detecting MS lesions, CSA region and CSA region without MS in axial spinal cord images as a result of FractalSpiNet.

created by obtaining MR data of MS lesions in the spinal cord and spinal cord region with a retrospective study. Dataset used in this study were obtained from a total of 87 patients diagnosed with MS within the last 2 years until May 2024, without patient definition. Of the 87 patients, 68 were female and the remaining 19 were male. The age range of the patients varied between 14 and 72 years. MR scans of the patient group were performed on a Siemens Magnetom Spectra 3.0T MR scanner. The data were collected using 2D MR slices in the T2-w modality in the turbo spin echo sequence, scanned from the axial (transverse) angle of the cervical spinal cord region, requested from MS patients as part of clinical routine. The slice thickness for MR slices in the scans in the dataset is 4 mm and there are between 24 and 30 slices in a scan. Since the spinal cord and lesions within these boundaries

are detected from axial planes of cervical spinal cord as in the study, MR images from the cervical region of the spinal cord, where MS lesions are more commonly observed, were used instead of the entire spinal cord [39]. In addition, the original dataset prepared for the automatic segmentation of the cervical spinal cord and cervical MS lesions in this study is publicly available from Mendeley Data.[1]

The acquisition parameters and other technical details for the dataset are given in Table 1.

The MR slices in the dataset were provided in DICOM format, which is widely used in medical imaging, and were converted to NIfTI format during the pre-processing steps. The ITK-Snap software tool [40] was used for data

[1]https://data.mendeley.com/datasets/ydkrtmygjp/1

TABLE 1. Technical Details and Acquisition Parameters in Axial (Transversal) Plane MR Scans For Original Dataset.

Number of subjects	87
Distribution of patients by gender	68 Female, 19 Male
Patient's age range	14-72
Scanner information	SIEMENS Spectra Magnetom
Sequence (scan mode)	2D
Series description	T2_TSE_TRA
Modality	Transversal T2-w imaging
Magnetic strength (T)	3.0
Slice thickness (mm)	4
Repetition time (ms)	3420
Echo time (ms)	86
Imaging frequency	123.185655
Spacing between slices	5.2
Percent sampling	90
Percent phase field of view	78.125
Pixel bandwidth	260
Flip angle (FA)	150
Dimensions	320x250 pixels
Number of slices	24–30
Ny, NEX	239, 3.00
Voxel spacing	0.6875x0.6875x 5.2

conversion. The MR scans in the dataset were reviewed by two different radiologists, and the ground truth mask creation processes were performed manually in the ITK-Snap environment, and the selected slices were double-checked and verified. An example of MR data masking of the spinal cord region and the MS lesion detected in this region for axial data using ITK-Snap software is shown in Fig. 2. Fig. 2(a) shows the axial plane MR image of the cervical spinal cord, and Fig. 2(b) shows the CSA region delineated and the MS lesions identified by experts with a concensus for ground truth masking. In this study, for the cervical spinal cord dataset, ground truth masks were created by consensus of two radiologists on MR slices. The first label indicates the area of the MS lesion in the CSA region, while the other label identifies the remaining area (CSA without MS) after subtracting the MS lesion from the CSA region. The grey area in Fig. 2 was not labelled.

When the cervical spinal cord is examined from the sagittal plane approximately along the C1-C7 vertebrae, each slice taken in the horizontal plane corresponds to axial MR data. In Fig. 3, each slice in axial planes was expertly controlled separately to determine which slices contained MS lesions. Masking of the slices with MS lesions was then performed, and masking of the entire dataset was completed by performing the same steps for all MR data. The dataset contains axial spinal cord boundaries and ground truth masks of MS lesions in this region. Since the spinal cord boundaries and MS lesions within these boundaries are detected in the study, there are 25 slices in average in the existing axial MR scans, and since MS lesions are observed in an average of 3 of these slices, ground truth labelling of spinal cord and MS lesions was performed only for these slices. On the MR slices in the dataset, MS lesions in the cervical spinal cord are located paracentrally in the caudal parts and peripherally in the posterior paramedian areas. As a result, a total of 231 MR slices and masks were obtained from all MR scans of 87 MS patients.
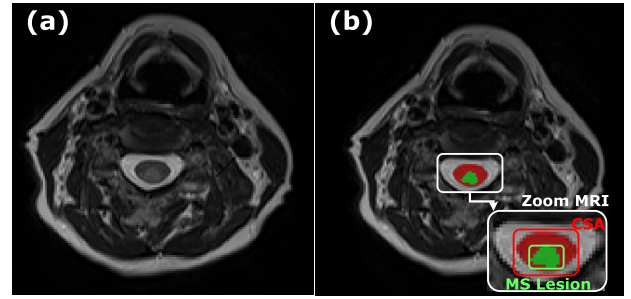
FIGURE 2. (a) Axial plane MR image of the cervical spinal cord and (b) spinal cord boundaries (cross-sectional area) and ground truth mask of MS lesions within this area delineated by the expert.

As MR technology does not yet allow zooming into the desired area, the slice of interest is obtained by general scanning. In this study, in order to eliminate the unnecessary background of the MR slices in the dataset and to increase the performance of the study, the data were resized and saved in.png format by cropping and rescaling operations based on the mask centre in the Python environment. The resizing process is considered as a stage that can significantly affect the success of the training

B. DATA ORGANIZATION
In the study, axial slices obtained from the MR scans were evaluated by experts and a dataset of spinal cord images with MS lesions was created. In data pre-processing shown in Fig. 4, a series of pre-processing steps were applied to organize the MR slices from 87 subjects in the dataset. In the first step of data preparation, axial planes from multiple DICOM images were identified. These images were re-registered in.nii format as NIfTI file. Subsequently, from these MR scans, 231 suitable sections from these MR scans were obtained in.png format in a second step, preserving their original size. In the third step, the region of the spinal cord was cut to 128×128 by cutting from the slices with 320×250 resolution. Here, the cervical spinal cord and MS areas in this region were manually masked by experts using ITK Snap software. Thus, the MR images were pre-processed for resampling and cropping to ensure that the images were of the same size. In our study, the size of the preprocessed MR slices was resized from 320×250 to 128×128. The reason for this is that in our study, we worked only in the CSA region of the cervical spinal cord axial plane MR slices. The regions outside the CSA are not region of interest (RoI) for us. Therefore, the CSA regions are automatically found in MR slices and the input images are resized, and since no resizing process is applied for the CSA region, there is no loss of essential features. In addition, in our study, data augmentation is applied to the resized images, making the proposed method robust for low resolution images.

As the total number of cross slices in the dataset was quite small, data augmentation was used to increase the available dataset in forth step of pre-processing and data organization. Data augmentation is a process to improve the variety and quantity of a limited dataset [41], [42]. In general, data
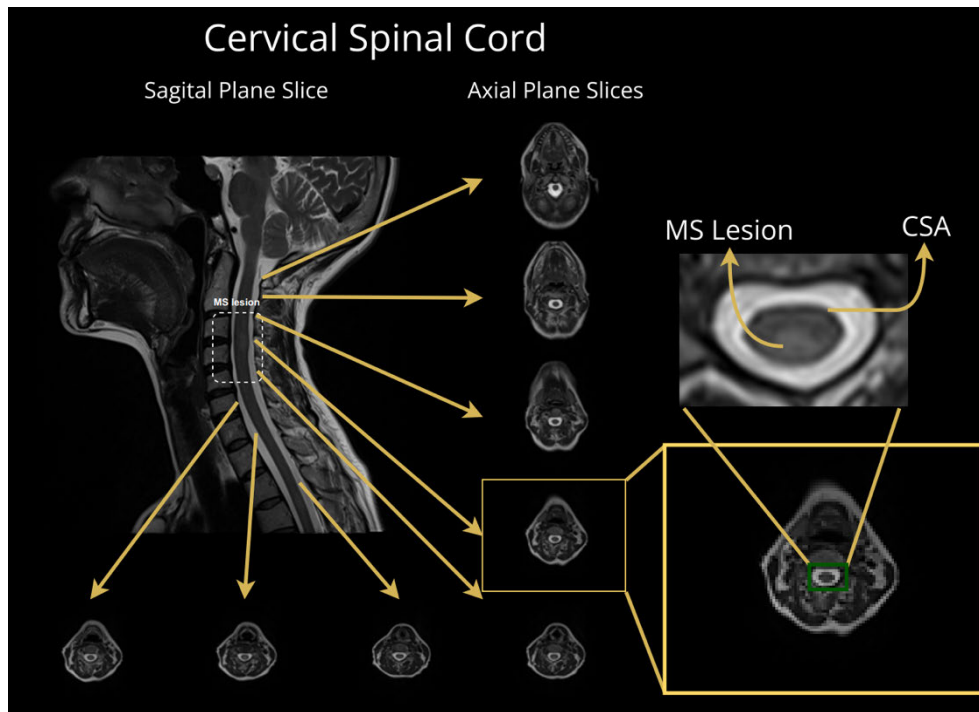
FIGURE 3. Axial plane slices of the spinal cord along the cord in the sagittal plane and the mask of those with MS in these axial plane slices and zoomed MRI of the mask.
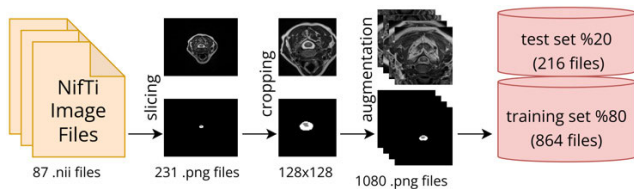

FIGURE 4. Pre-processing steps and data augmentation of the existing dataset and separation of data into test and training.

augmentation is applied when the desired number of data cannot be obtained in the field of medical image processing. In this study, the most important factor providing data diversity is that the structure, shape and size of the spinal cord and MS lesions are different in each scan. Although this is the most challenging part of the study, both the unique shape of the spinal cord region and the different locations and sizes of the MS lesions are the most important factors in the diversity of the dataset. In this study, for data augmentation, the NumPy library functions rotation (*in x and y axes*), flipping, shift and same were used. As part of the study, the total number of images in the dataset was increased from 231 to 1080 using the procedures shown in Fig. 4.

C. PROPOSED METHODOLOGY

In the field of deep learning, many models have been developed from the past to the present, and convolutional deep networks are the most popular in this sense. Thanks to its adjustable parameter structure, convolution allows the development of deeper networks [43], [44]. It has often been used as the most basic model in deep network structures, thanks to its ability to detect higher-valued features than simple features throughout the convolutional layers. In fact, with the development of the U-Net architecture in the field of medical imaging using this convolutional structure, it has become very widely used. The U-Net architecture is widely used by researchers in many fields other than medical imaging. In this study, FractalSpiNet architecture, a fractal convolution-based hybrid U-Net model, is proposed for the detection of cervical spinal cord and MS lesions.

1) U-NET

The U-Net architecture was firstly developed for biomedical imaging applications [45]. It has become very popular among image segmentation methods due to its structure and performance [46]. Thanks to the flexibility of the U-net architecture, whose typical structure is shown in Fig. 5, to evolve into different models (U-shaped), mixed models or new U-models with new layer connections can be developed by using the block structures of other deep learning models or the proposed convolutional models. The success of classical convolutional neural network models is directly proportional to the size of the dataset. This is because the images in the datasets are labelled, feature maps are extracted and supplied to the model, and the model performs operations by identifying this data from the label information. Unlike other deep learning models, U-Net can achieve faster results with fewer datasets thanks to its context-based learning feature [47].

In addition to the effective learning capability of the base model, the different layer connections of the hybrid models provide more different feature sets. This is achieved by preserving the features that characterise the data within the layer structure. In this way, the new U-Net hybrid models contribute positively to the performance value obtained from the model.

The U-Net deep learning architecture consists of two symmetric parts, an encoder and a decoder, connected by a bottleneck [48]. Convolutional operations are applied in the direction of downward contraction (encoder) and upward expansion (decoder) [49]. The downstream coding block consists of twice 3×3 convolution operations, ReLu activation and 2×2 maximum pooling operations for downstream transmitted data [50]. At this stage, batch normalization, which is not used in the classical U-Net architecture, can be integrated into the model. Batch normalisation is a widely used technique that allows Deep Neural Networks (DNNs) to train the model faster and more stable by keeping the optimisation in the training process as smooth as possible [51]. As a result of these operations, one output, obtained as a result of convolution activation and batch normalisation, is given as input to the decoder block, while the other output, which is subjected to maximum pooling, is sent to a lower layer. These processes are applied sequentially at a lower level along each layer. This is the most important feature of the U-Net architecture, which combines low-level features from the encoder path with the high-level representation derived from the decoder path to enrich the localisation information [52]. The downstream data size is halved while the filter size is doubled. Downward convolution is followed by upward inverse convolution and ReLu activation is applied. In addition, the expansion path increases the resolution of the output, which then provides data to the final convolutional layer to produce a fully segmented image. The fully connected layer structure often used in convolutional models is not used in the U-Net architecture, instead class mapping is performed at the end of the model using a 1×1 convolution. The success of the model is obtained by evaluating the results with pixel-based similarity metrics between the output and the input.

2) FRACTAL NETWORKS

Mandelbrot expresses fractal geometry as a statistical quantity that expresses fractal dimensionality. It is defined as a set formed as a result of the formation of a whole by a series of shapes that are similar in themselves, i.e. with self-similarity [53], [54]. This set is called the ''Mandelbrot set''. In fractal geometry, each part is a linear geometric reduction of the whole, with the same reduction ratios in all directions and adds ''the parts, no matter how small, are similar to the whole''. In other words, fractals can be expressed in terms of an infinitely expandable unity that has the similarity of the fundamental particle. Within this represented wholeness, each part carries the essential part of the fractal. The Mandelbrot set seen in Eq. (1) is formed by squaring the parameter
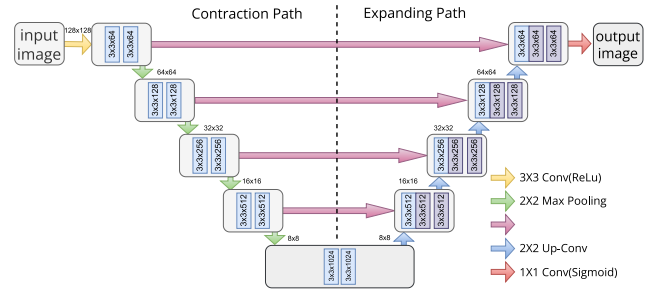
FIGURE 5. The typical architecture of the U-Net deep learning network used in this study for automatic segmentation of the spinal cord and deduction of MS lesion.

z of the function $f(z)$ in the plane of complex numbers and adding a fixed number [53]. In fact, it is concluded that different complex fractal structures can be created with very simple mathematical equations or iterative processes.

$$f(z) = z^2 + c \tag{1}$$

It is very important to develop deep networks in convolutional architecture. The transversal and longitudinal expansion feature of the fractal structure has been very inspiring to develop a convolutional model [55]. In this context, there is a convolutional model developed using the fractal structure [56]. As shown in Fig. 6(a), in the convolution block structure inspired by fractal geometry, a single convolution structure between input and output is expressed as $f_c(z)$. Each expansion is denoted by $f_{c+1}(z)$. From bottom to up as seen in Fig. 6 (c), columns nested by C have a convolution structure of 2^{C-1}. It is possible to deepen the network as many times as the fractal convolution block between each input and output layer [56]. The expression in Eq. (2) is used for the fractal convolution structure, while Eq. (3) is used for the custom fractal structure.

$$f_c(z) = conv(z) \tag{2}$$
$$f_c(z) = conv(z) + BN(z) + Activation\ ReLu(z) \tag{3}$$

The expanding convolution structure within the fractal convolution allows for a deeper architecture configuration. The main advantage of this approach is that the output features can be applied to datasets with different resolution values, scaled rather than absolute values [57]. As shown in Fig. 6 (b) and Fig. 6(c), the block structure of the architecture expands by 2^n at each step and each of them is connected by different sub-paths. Such an expansion of the fractal structure shows that an extremely deep convolutional network structure can be obtained.

3) FractalSpiNet

For the development of new U-Net architectures, it is possible to contribute skip connection enhancements, backbone design enhancements, bottleneck enhancements, transformers, rich representation enhancements, probabilistic design [52]. Thus, in this study, a U-Net configuration with different convolutional layer structure is proposed for a new
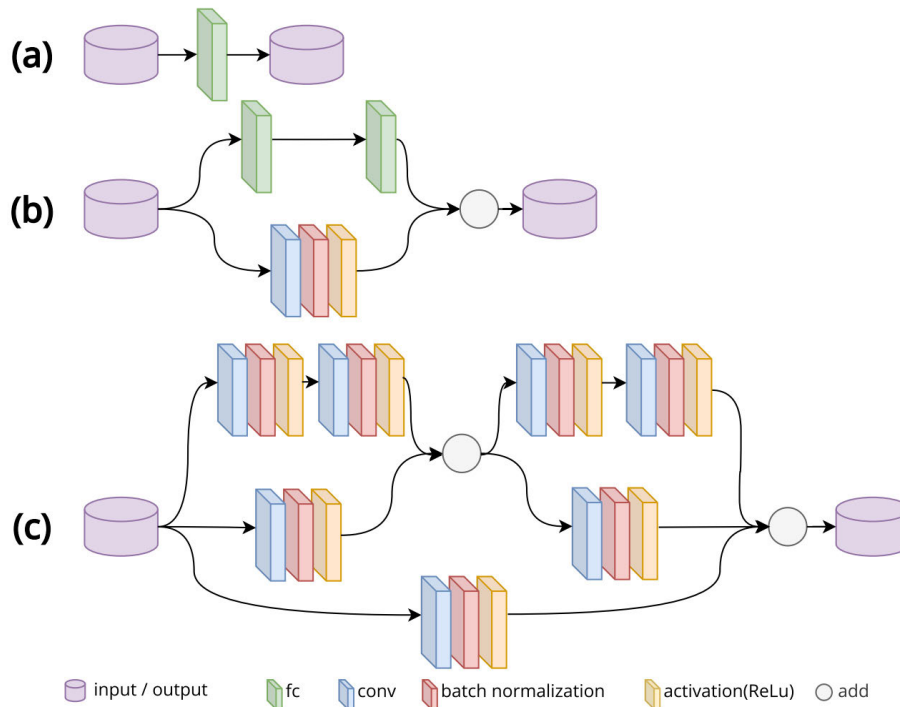
FIGURE 6. Fractal convolution structure progresses from simple to expanding structure in the order a, b, c. FractalNet convolution base structure $f_C(z) = conv(z)$ (a), the fractal structure, which expands with a convolution of 2^{C-1}, is shown in b in the 2nd expansion, c in the 3rd expansion. As seen in c, each convolution block is designed as a convolution, batch normalization and ReLu activation function.
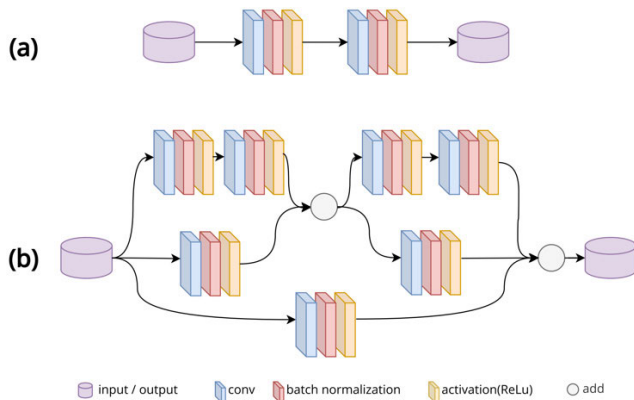
FIGURE 7. U-Net and FractalSpinet convolution block structure. (a) In the original U-Net by Ronneberger et al. [46], each level in the encoder consists of two 3 × 3 convolutional layers with batch normalization and ReLu activation, (b) FractalSpiNet convolution block structure which expands with a convolution of 2^{C-1}.

backbone design enhancement. It is also possible to design different deep network models with different number of layers and block structures in the U-Net architecture. In this study, a new hybrid model FractalSpiNet was developed for cervical spinal cord segmentation and MS lesion detection using the fractal convolution structure shown in Fig. 7 instead of the sequential/regular convolution used in the encoder and decoder blocks in the U-Net model. Fractal convolution is a concept in deep learning to enhance feature extraction by

leveraging fractal structures. Regular convolution identifies specific features present in a small area of the image, while fractal convolution can identify features that repeat at different scales within the image. Therefore, fractal convolution leverages the principles of fractals to capture multi-scale features efficiently, providing a larger receptive field and potentially reducing the complexity of the network. Fig. 7(a) shows the U-Net convolution block structure with batch normalisation and Fig. 7(b) shows the proposed FractalSpiNet convolution block structure. In the FractalSpiNet model, the convolution used in the encoder and decoder blocks is extended to add depth to the U-Net architecture. The code of the proposed FractalSpiNet architecture is publicly available on GitHub.[2]

In order to keep the depth of the fractal structure integrated into the U-Net architecture at an optimal level, the FractalSpiNet structure in Fig. 8 was designed considering the benefit-loss relationship. In the benefit-loss relationship, the model was evaluated according to its contribution to the key metric performances obtained during the training period. In fact, it is possible to extend the network as much as desired, but designing the deepest network does not always give the optimal result for the model. In this context, the number c in the convolution structure, up to 2^{C-1}, determines the depth of the network. The fractal structures embedded in the coding blocks are downsampled and upsampled in the decoder

[2]https://github.com/BSEU-Misal/FractalSpiNet
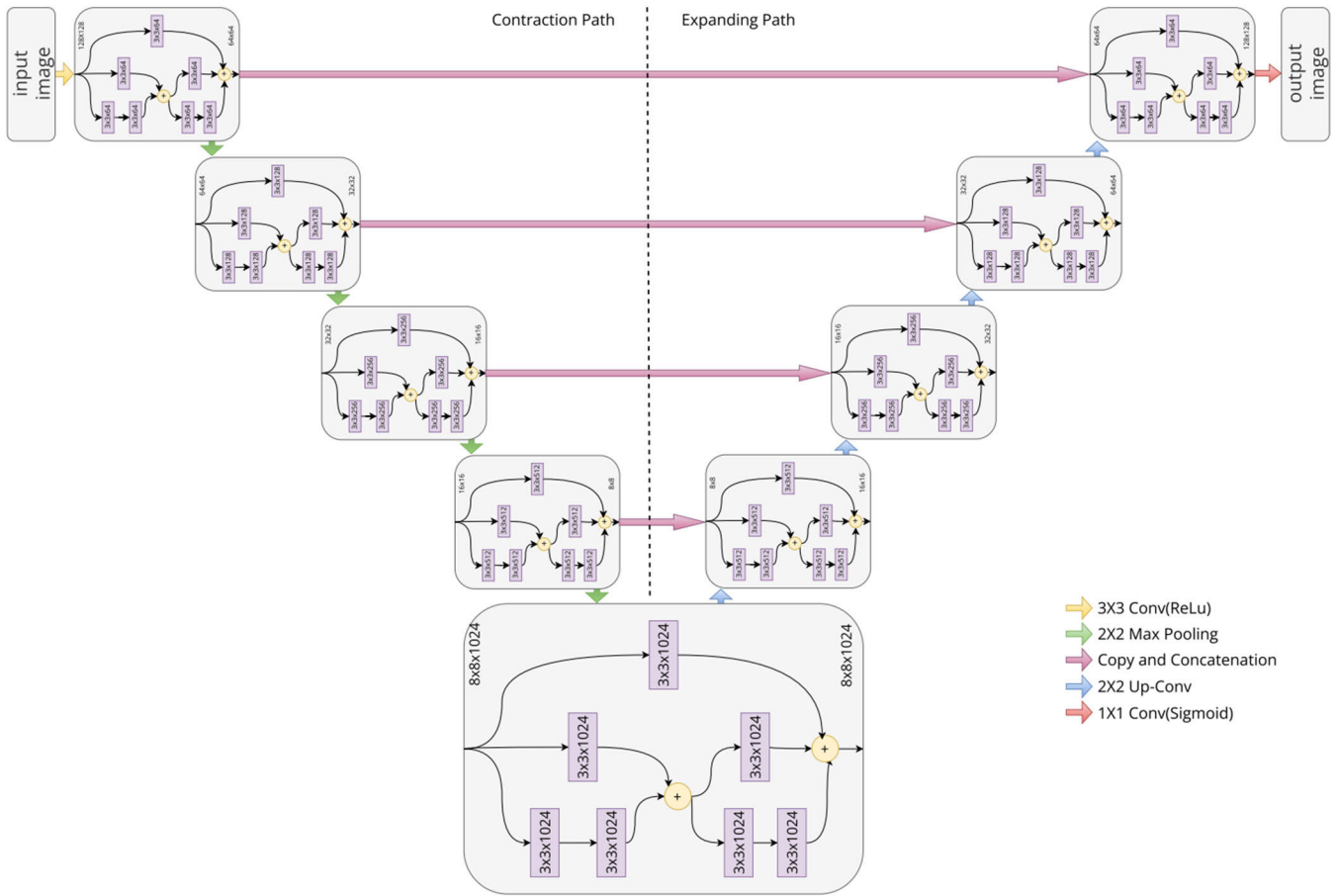
FIGURE 8. The proposed architecture of the FractalSpiNet for segmentation of cervical spinal cord and MS lesions on MR scans.

direction to create a segmentation mask for the input images. As in the classical convolution block structure, the fractal convolution block is used as a convolution batch normalisation and ReLu activation. In the FractalSpiNet architecture, the processing steps of the model are the same, but the convolution structure of the model is changed and the contribution of the newly proposed convolution block to the model is taken into consideration.

IV. EXPERIMENTAL AND RESULTS
In this study, the FractalSpiNet hybrid architecture was developed for automatic segmentation of the cervical spinal cord region and detection of MS lesions in the cervical spinal cord using a new dataset consisting of axial plane T2-w MR slices. In the experimental studies, the ITK-Snap software was used to examine the original MR data and perform masking, while the Python programming language and the Jupyter Notebook IDE, commonly used in deep learning studies, were used for network training and evaluation of results. A computer with Intel Core i5 4.10 GHz CPU, 16 GB DDR4 3000 MHz RAM, NVIDIA RTX A4000 16 GB GPU and 1TB HDD together with 500 GB SSD disc hardware was used for all experimental studies in the study.

In this study, the performance of the proposed Fractal-SpiNet method for automatic segmentation of the cervical spinal cord region and detection of MS lesions in the cervical spinal cord is compared with state-of-the-art methods such as Attention U-Net (Att U-Net), Residual U-Net (Res U-Net) and Attention Residual U-Net (Att-Res U-Net), especially typical U-Net. Unnecessary areas like background in the images are ignored when segmenting the region of interest using the Att U-Net architecture [58]. By using only the relevant areas during training, this architecture reduces the computational cost and improves the generalisation of the network. In the Res U-Net model, the convergence problem of deep networks is solved and the success of model training is increased by adding the connection structures used in CNN structures to the convolution blocks in the U-Net model [59]. Thus, it can progress faster in the deep network structure with residual connection structures. In the Att-Res U-Net architecture, the attention mechanism and residual blocks are used together in the U-Net architecture [60].

In our study, in the preliminary experimental analyses with only 231 images in the dataset, DSC scores of 91.02%, 90.50%, 89.62%, 90.12% and 85.69% were obtained for the proposed FractalSpiNet, U-Net, Att U-Net, Res U-Net and

TABLE 2. The Training Times And The Number Of Parameters At The End Of Training For The Proposed Fractalspinet And Other State-Of-The-Art Methods.

Method	Training time (Min:Sec)	Total parameters for method
U-Net	28:37	31.401.349
Att U-Net	35:19	37.333.513
Res U-Net	33:47	33.156.933
Att-Res U-Net	40:50	39.089.097
FractalSpiNet	91:18	109.922.693

TABLE 3. Optimization Of Hyperparameters Used in the Training of U-Net and FractalSpiNet Networks.

Hiperparameter	Value
Epoch	200
Batch size	8
Learning rate	0.001
Dropout	0.5
Activation function	ReLU
Output activation function	Sigmoid
Optimization algorithm	Adam
Loss function	Binary cross entropy

Att-Res U-Net for segmentation of the CSA region without MS lesions, respectively. On the other hand, for the detection of MS lesions in the cervical spinal cord, DSC scores of 63.64%, 47.91%, 50.34%, 52.57% and 30.11% were obtained with the same models, respectively. Therefore, since the results obtained for the data set were not satisfactory, data augmentation was applied to the dataset. In the experimental studies with data augmentation, 864 (%80) of the images were used for training and the remaining 216 (%20) were used for test in a dataset consisting of 1080 images. In addition, our study used data augmentation to increase the number of images in the dataset from 231 to approximately 5 times to reduce the overfitting effect. This exploits the learned features from the larger dataset and improves performance on smaller datasets. Table 2 shows the training times and the number of parameters at the end of training for the proposed FractalSpiNet and other state-of-the-art methods for a total of 200 epoch. Since the number of parameters computed for FractalSpiNet is higher than the other models with 109.922.693, the training time is also higher with approximately 91 minutes. For the typical U-Net architecture, the number of parameters and the training time are about 3 times lower than for FractalSpiNet. Compared to FractalSpiNet, U-Net and other state-of-theart methods have a lower number of parameters, leading to faster training times and lower memory usage. However, FractalSpiNet's strength lies in its ability to capture complex features, potentially leading to superior performance on tasks involving intricate details or highly textured data.

In order to verify the performance of the FractalSpiNet architecture, the same hyperparameter values given in Table 3 were used to train the proposed FractalSpiNet architecture and other state-of-the-art U-Net models. The number of images in the dataset, which was 231, was increased approximately five times with data augmentation techniques. The number of epochs was set at 200 due to the large number of images used in the training sets to train the networks. The number of epochs is used in this way to emphasize that the results are compared under equal conditions in terms of evaluating the models with the same hyperparameter inputs. Batch size is an important parameter in the training of U-Net and models. Batch size=8 was used as a small cluster size as it optimizes the memory usage in the training process and increases the generalization ability of the models. On the other hand, a small batch size and learning rate=0.001 was

sufficient for the network to learn and generalize quickly. In the pre-analyses, dropout=0.5 was used in the training of the models to reduce the overfitting effect of the network. The ReLu activation function was used for segmentation, especially for U-Net based architectures, due to its non-linearity, sparsity and vanishing gradient reduction. Since multi-label segmentation was used in this study, Sigmoid was preferred as the output activation function. In addition, Adam was used as the optimization function because it is more effective in U-Net based segmentation and enhances adaptive learning. Furthermore, Binary Loss Function was chosen as the loss function because it is efficient in binary segmentation tasks and faster when used with the Adam optimization function.

The progress of training loss, training accuracy (training acc), validation loss and validation accuracy (validation acc) values obtained as a result of training the proposed FractalSpiNet architecture and other state-of-the-art U-Net models for segmentation of the cervical spinal cord and MS lesions along the cord using MR images in the dataset during 200 epochs is shown in Fig. 9 (a), Fig. 9 (b), Fig. 9 (c) and Fig. 9 (d). As can be seen from these change graphs, significant results are obtained for the training phase for the proposed FractalSpiNet architecture in terms of accuracy and validation values.

In the experimental studies, important key metrics were used to evaluate the performance of the segmentation of the cervical spinal cord region and the detection of MS lesions. One of them, the Dice similarity coefficient (*DSC*), shows the segmentation ratio between the ground truth and the prediction mask in Eq. (4). Other metrics, such as volumetric overlap error (*VOE*) in Eq. (5), Hausdorff distance 95 (*HD95*) in Eq. (6.1), (6.2) and (6.3), average surface distance (*ASD*) in Eq. (7) and relative volume difference (*RVD*) in Eq. (8), are often used to evaluate the segmentation results. On the other hand, it is possible to compute many evaluation metrics using confusion matrix values, including true positive (TP), false positive (FP), false negative (FN) and true negative (TN) [61]. Recall (*REC*) in Eq. (9) is the ratio of correctly predicted pixels by the model to the actual correct pixels, while Precision (*PRE*) in Eq. (10) shows how many of the values predicted as positive are actually positive. In the equations for the metrics used, PM (predicted mask) represents the segmentation result obtained by the proposed method, while GM (ground truth
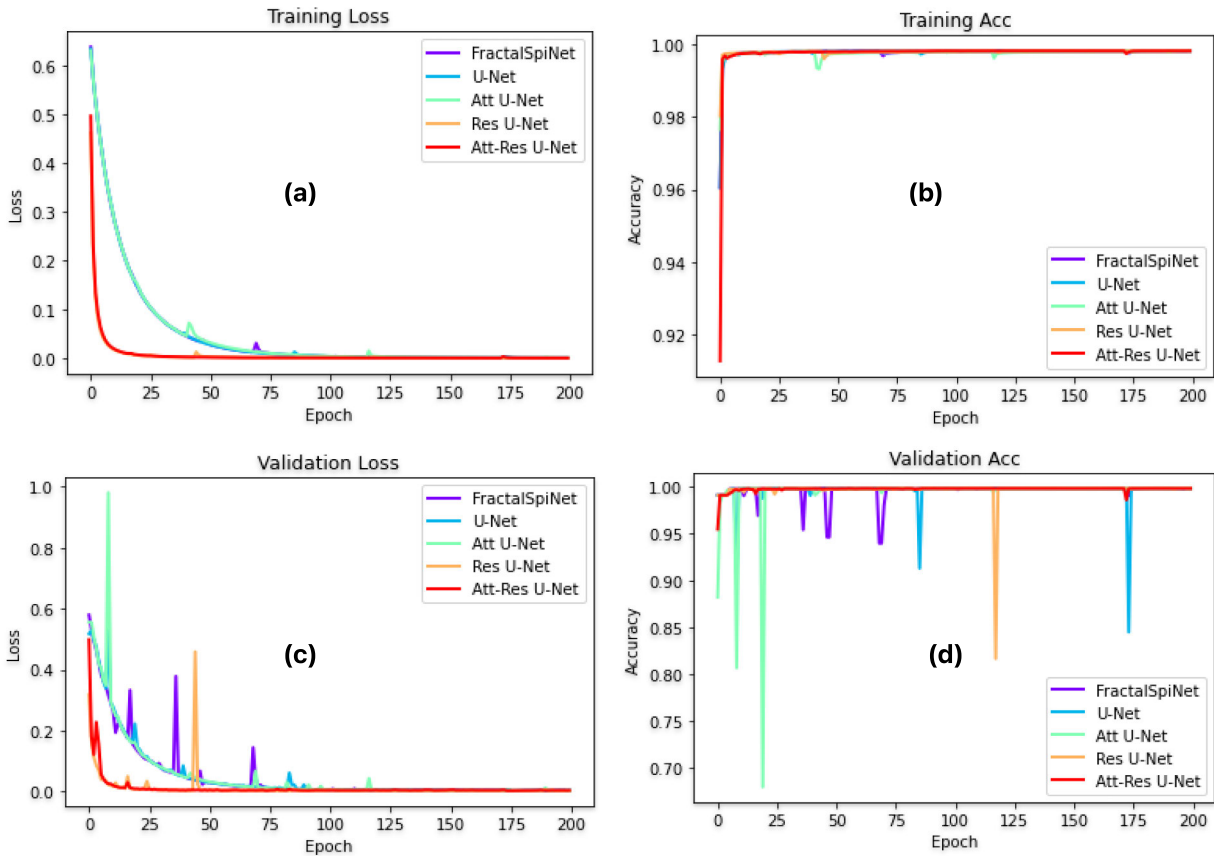
FIGURE 9. Development of (a) training loss and (c) validation loss and (b) training accuracy and (d) validation accuracy values for proposed FractalSpiNet architecture and other state-of-the-art models such as U-Net, Att U-Net, Res U-Net and Att-Res U-Net during 200 epochs of training (batch size=8).

mask) represents the reference area masked by the expert radiologist.

$$DSC(PM, GM) = \frac{2x\,|PM \cap GM|}{|PM| \cup |GM|}x100 \quad (4)$$

$$VOE(PM, GM) = (1 - \frac{|PM \cap GM|}{|PM| + |GM| - |PM \cup GM|})x100 \quad (5)$$

$$hd(PM, GM) = \max_{x \in PM} \min_{y \in GM} \|x - y\|_2 \quad (6.1)$$

$$hd(GM, PM) = \max_{y \in GM} \min_{x \in PM} \|x - y\|_2 \quad (6.2)$$

$$HD95(PM, GM) = \max(hd(PM, GM), hd(GM, PM)) \quad (6.3)$$

$$ASD(PM, GM) = \frac{1}{|s(PM)| + |s(GM)|} \times \left(\sum_{S_{PM} \in S(PM)} d(SPM, S(GM)) + \sum_{S_{GM} \in S(GM)} d(SGM, S(PM)) \right) \quad (7)$$

$$RVD(PM, GM) = (\frac{|PM| - |GM|}{|GM|})x100 \quad (8)$$

$$REC(PM, GM) = \frac{TP}{TP + FN}x100 \quad (9)$$

$$PRE(PM, GM) = \frac{TP}{TP + FP}x100 \quad (10)$$

The parameter values used in the training of the proposed FractalSpiNet architecture and other state-of-the-art models such as U-Net, Att U-Net, Res U-Net and Att-Res U-Net were trained with the same values and the effect of the model structure on the performance was evaluated. A number of results were obtained for the models as a result of training with the proposed FractalSpiNet and other architectures using the dataset specifically prepared for the study. Using these architectures, CSA segmentation of cervical spinal cord from the axial plane within the limits of the total cervical spinal cord area, segmentation without MS lesions within cervical spinal cord CSA from the axial plane, and detection of MS lesions in the cervical spinal cord CSA were achieved. Firstly, the predictive capabilities of the proposed FractalSpiNet model and others for segmentation of the spinal CSA in the axial plane within the boundaries of the whole cervical spinal cord area are shown in Fig. 10 with the DSC scores. Analysis of the sample images selected from the test set shows that all models produced segmentation results with very high DSC scores. Despite the high performance of all models, it can be seen that the DSC scores obtained with the proposed FractalSpiNet architecture are higher.

The results obtained for the proposed FractalSpiNet model and other state-of-the-art models such as U-Net, Att U-Net, Res U-Net and Att-Res U-Net architectures for the segmen-
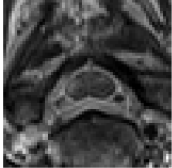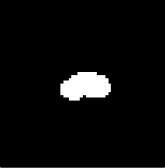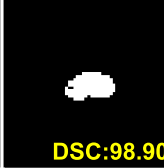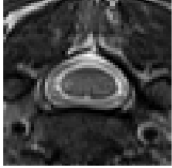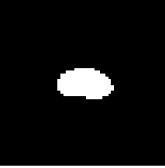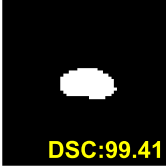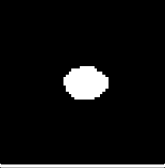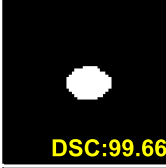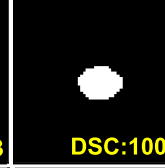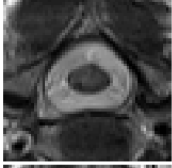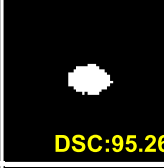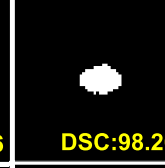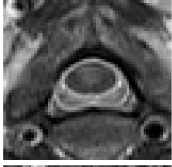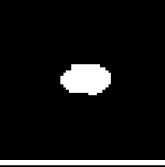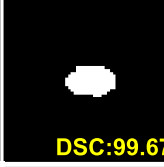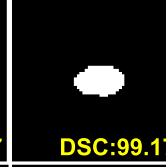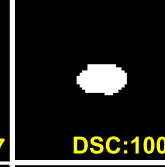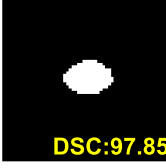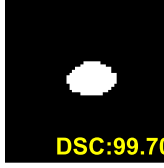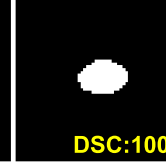
FIGURE 10. Results for segmentation of the CSA region in cervical spinal cord for the proposed FractalSpiNet and other state-of-the-art models.

tation of the spinal cord CSA in the axial plane within the boundaries of the entire cervical spinal cord area are shown in Table 4. Here, all key metric values are obtained individually for all images in the test dataset, and the segmentation results of the spinal cord area are calculated separately. The segmentation success is obtained by averaging the metric results calculated for each MR slice and the results are reported in detail. For the models, the same values were given for all training parameters and the training performance was evaluated for 200 epochs. All values were calculated by averaging the segmentation successes for the MR slices forming the test set. A detailed analysis of Table 4 shows that the FractalSpiNet results are more successful in segmenting the CSA region in cervical spinal cord. The DSC scores obtained using the proposed FractalSpiNet architecture are 98.88% for the CSA region in whole spinal cord, while the DSC scores for U-Net, Att U-Net, Res U-Net and Att-Res U-Net models are 98.54%, 98.01%, 98.67%, and 97.90%, respectively. In addition, the results of distance-based metrics

such as HD95 and ASD were also confirmed to be more successful with the proposed FractalSpiNet, with smaller distances being achieved. Furthermore, it can be seen from the key metric results that the most successful model after the proposed FractalSpinet architecture is the Res U-net, although for some metrics the U-net is more successful.

The prediction results of the proposed FractalSpiNet, U-Net, Att U-Net, Res U-Net and Att-Res U-Net architectures for segmentation of MS lesions within the boundaries of the cervical spinal cord area are shown in Fig. 11 with the DSC scores. Analysis of sample images selected from the test set with ground truth delineated by experts shows that MS lesions are detected with high DSC scores. Although the detection of MS lesions in this small area is a very challenging task, very high scores were obtained. The proposed Fractal-SpiNet architecture achieved higher scores on average than other state-of-the-art U-Net architectures in the detection of MS lesions in cervical spinal cord. In the segmentation of MS lesions with the proposed FractalSpiNet architecture, there
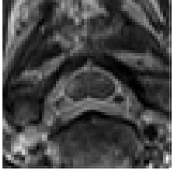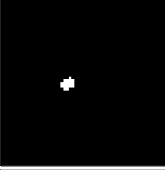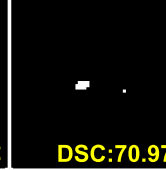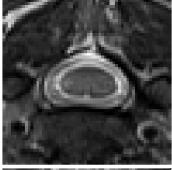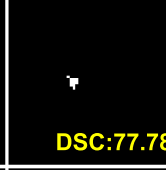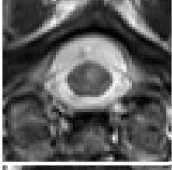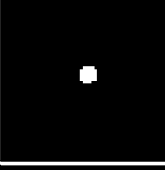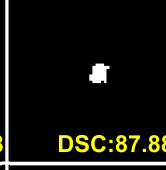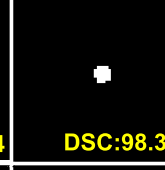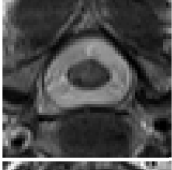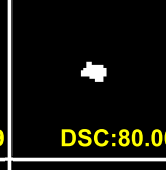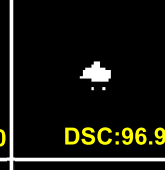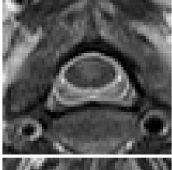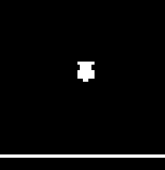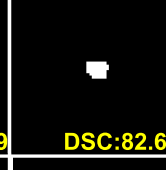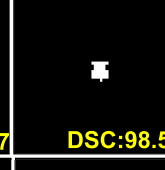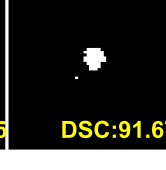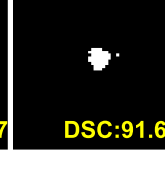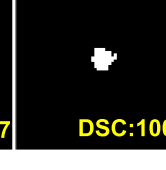
FIGURE 11. Comparison of state-of-the-art methods and the proposed FractalSpiNet architecture in segmentation of MS lesions in cervical spinal cord area.

is no artefact around the lesion, whereas in the segmentation with the other methods U-Net, Att U-Net, Res U-Net and Att-Res U-Net, there are large and small pieces.

The performance results of the proposed FractalSpiNet and other state-of-the-art models such as U-Net, Att U-Net, Res U-Net and Att-Res U-Net architectures in the detection of MS lesions in the cervical spinal cord region is shown in Table 5. The segmentation results of MS lesions for all MR images in the test set were measured separately for all models. The segmentation success is obtained by averaging the metric results calculated for each MR slice, and the results are presented in detail based on the key metric. It is seen that the proposed FractalSpiNet method is more successful and detects MS lesions in all slices in the test set with a DSC score of 90.90%. The DSC values obtained for other state-of-the-art models such as U-Net, Att U-Net, Res U-Net and Att-Res U-Net for segmentation of MS lesions in the cervical spinal cord are 86.0%, 75.34%, 88.87% and 83.06%

respectively. On the other hand, the proposed FractalSpiNet architecture has a lower error for VOE, which is used to measure the overlap error in segmentation tasks. Moreover, for HD95 and ASD, which are distance-based key metrics in segmentation, FractalSpiNet achieves better performance with 8.08 mm and 16.08 mm, respectively. According to the proposed FractalSpiNet architecture, the Res U-Net model appears to be more successful in segmenting MS lesions in the cervical spinal cord. Furthermore, for the remaining key metrics RVD, REC and PRE, the FractalSpiNet architecture has better performance in segmentation of MS lesions in the cervical spinal cord.

The CSA region without MS lesion is one of the two labels delineated by experts on the images in the dataset. This label represents the CSA region without an MS lesion in the cervical spinal cord, if present. Segmentation of this area allows detection of the remaining non-MS spinal cord area, despite the difficulty in detecting MS lesions. Thus, MS lesions

TABLE 4. Results Obtained for The Proposed FractalSpiNet and Other State-of-the-art Methods for Axial Plane Spinal Cord CSA Segmentation.

KEY METRIC	METHODS				
	U–Net	Att U–Net	Res U–Net	Att-Res U–Net	FractalSpiNet
DSC (%)	98.54	98.01	98.67	97.90	98.88
VOE (%)	2.67	3.64	2.43	3.90	2.04
HD95 [mm]	0.49	1.36	0.60	1.32	0.39
ASD [mm]	1.67	3.90	1.55	3.68	1.38
RVD (%)	1.51	2.71	1.55	2.19	0.97
REC (%)	98.43	98.80	98.69	98.59	98.84
PRE (%)	98.69	97.33	98.70	97.26	98.94

TABLE 5. Performance Of Proposed FractalSpiNet Architecture and Other State-of-the-art Methods in Segmentation of Cervical Spinal Cord MS Lesions.

KEY METRIC	METHODS				
	U–Net	Att U–Net	Res U–Net	Att-Res U–Net	FractalSpiNet
DSC (%)	86.00	75.34	88.87	83.06	90.90
VOE (%)	20.83	36.18	17.20	25.58	14.06
HD95 [mm]	11.55	21.92	9.83	14.28	8.06
ASD [mm]	28.23	67.98	31.28	47.47	16.08
RVD (%)	13.50	24.52	11.29	15.37	9.62
REC (%)	83.73	69.56	90.24	85.11	91.26
PRE (%)	90.50	85.25	89.33	83.04	92.20

can be detected with binary validation. In the experimental studies, the results of the proposed FractalSpiNet, U-Net, Att U-Net, Res U-Net and Att-Res U-Net architectures were also compared for segmenting the CSA region without MS lesions within the boundaries of the cervical spinal cord area. As can be seen in Fig. 12, analysis of the sample MR images selected from the test set shows that segmentation is achieved with higher DSC values using the proposed FractalSpiNet architecture, although the segmentation results are close to each other.

In addition, Table 6 shows the segmentation of the spinal cord CSA region without MS lesion for proposed Fractal-SpiNet, U-Net, Att U-Net, Res U-Net and Att-Res U-Net architectures and the detailed comparison of the segmentation results obtained based on the key metrics. It can be concluded that the proposed FractalSpiNet method outperforms U-Net architecture in terms of segmentation performance for all key metrics. Proposed FractalSpiNet, U-Net, Att U-Net, Res U-Net and Att-Res U-Net architectures achieved scores of 97.17%, 96.18%, 94.42%, 96.64% and 94.50% for DSC in spinal cord CSA region without MS lesion segmentation, respectively. Following the proposed FractalSpiNet architecture, the Res U-Net model is more successful in spinal cord CSA region without MS lesion segmentation.

V. DISCUSSIONS

When the results obtained as a result of the experimental analyses are examined in detail, it can be seen that the results obtained by using the proposed FractalSpiNet and other state-of-the-art models such as U-Net, Att U-Net, Res U-Net and Att-Res U-Net are more successful in finding both the entire cervical spinal cord area and the spinal cord area of the MS lesion compared to the MS lesion detection. The DSC values obtained using the proposed FractalSpiNet architecture show a score of 98.88% for full CSA area in the whole spinal cord, while detecting the spinal cord area without considering the MS lesion is 97.17%. On the other hand, using the proposed

FractalSpiNet architecture for the detection of MS lesions, a DSC score of 90.90% was achieved, comparing to other models. Considering the fact that MS lesions are expressed with very small pixels and do not have a specific geometric shape, it can be said that the proposed FractalSpiNet architecture also performs very successful segmentation and achieves remarkable results.

In general, MS lesions keep a very small area in the axial spinal cord slice. Although the detection and segmentation of these lesions is a very challenging process, it is seen that the proposed FractalSpiNet method can detect MS lesions with high accuracy even in MR slices with very small MS lesions. However, it is an inference obtained as a result of the training that the most important detail here is whether the areas with MS lesions are clearly defined in the original MR data. In fact, the areas with similar polarities to the MS lesions in the MR data reduce the success and make it very difficult to prepare the mask data (ground truth) at the very beginning of the process steps. Therefore, it is very likely that the proposed study will contribute to the detection of MS lesions in high quality clear MR slices.

On the other hand, in the segmentation results of some MR slices in the test set, it was observed that the boundaries could be overflowed by small scales or an incomplete segmentation prediction could be performed, although very rarely. Fig. 13 shows some examples of less successful results for the proposed FractalSpiNet architecture and other state-of-the-art models such as U-Net, Att U-Net, Res U-Net and Att-Res U-Net. Fig. 13 (a) shows the segmented CSA area in the spinal cord with a lower DSC score compared to the ground truth mask delineated by experts. Comparing the FractalSpiNet architecture with other state-of-the-art models such as U-Net, Att U-Net, Res U-Net and Att-Res U-Net for the same MR slice, the proposed FractalSpiNet architecture has a less successful segmentation result than the average for full CSA, while here it is more successful than the others
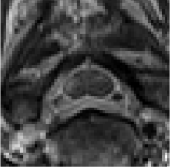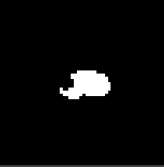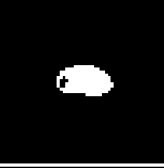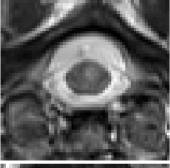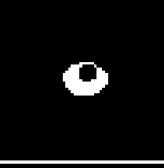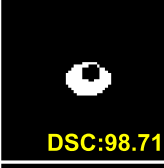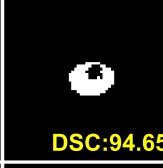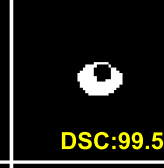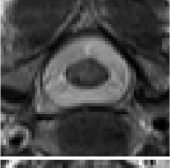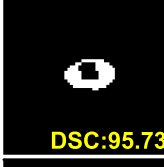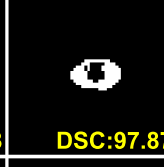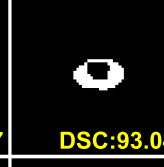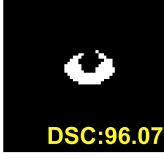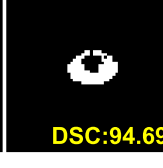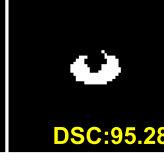
FIGURE 12. Segmentation of the spinal cord CSA region without MS lesions and key metric-based performance comparisons for the proposed FractalSpiNet architecture and other state-of-the-art methods.

based on the DSC score. Fig. 13 (b) shows the segmentation of the spinal cord region without MS lesion, which has a lower DSC score than the average. In this segmentation, the proposed FractalSpiNet architecture is more successful than other state-of-the-art methods. On the other hand, Fig. 13 (c) shows visualisations for less successful segmentation results compared to the average for the detection of MS lesions in the CSA region. In addition, the segmentation performance in the detection of MS lesions is lower than the segmentation of the CSA region and the CSA region without MS lesions. One of the reasons for some of these less successful segmentation and detection results is thought to be that the boundaries with polarities similar to the MS polarity in the MR data as a result of network training can be evaluated as MS in the prediction phase of the models. On the other hand, although lower than average results were obtained in the segmentation of MS lesions in the CSA region, a higher DSC score was obtained using the proposed FractalSpiNet

architecture compared to other state-of-the-art U-Net, Att U-Net, Res U-Net and Att-Res U-Net models.

In this study, the performance of the FractalSpiNet model based on the U-Net deep learning architecture, proposed for automatic segmentation of the CSA region of the cervical spinal cord and MS lesions in the CSA region, was also evaluated on the Spinal Cord Grey Matter Segmentation Challenge [62], a publicly available dataset. In order to have a more meaningful and fair evaluation and comparison of this study, this spinal cord dataset was used. This dataset consists of spinal cord images from four different sites. A total of 411 MR images and ground truth masks, including 328 training (~80%) and 83 test (~20%) sets, were selected from this dataset for experimental analysis. In addition, to verify the performance of the proposed FractalSpiNet architecture on this dataset, the previously proposed state-of-the-art methods were compared with U-Net and its derivatives, Att U-Net, Res U-Net and Att-Res U-Net models.
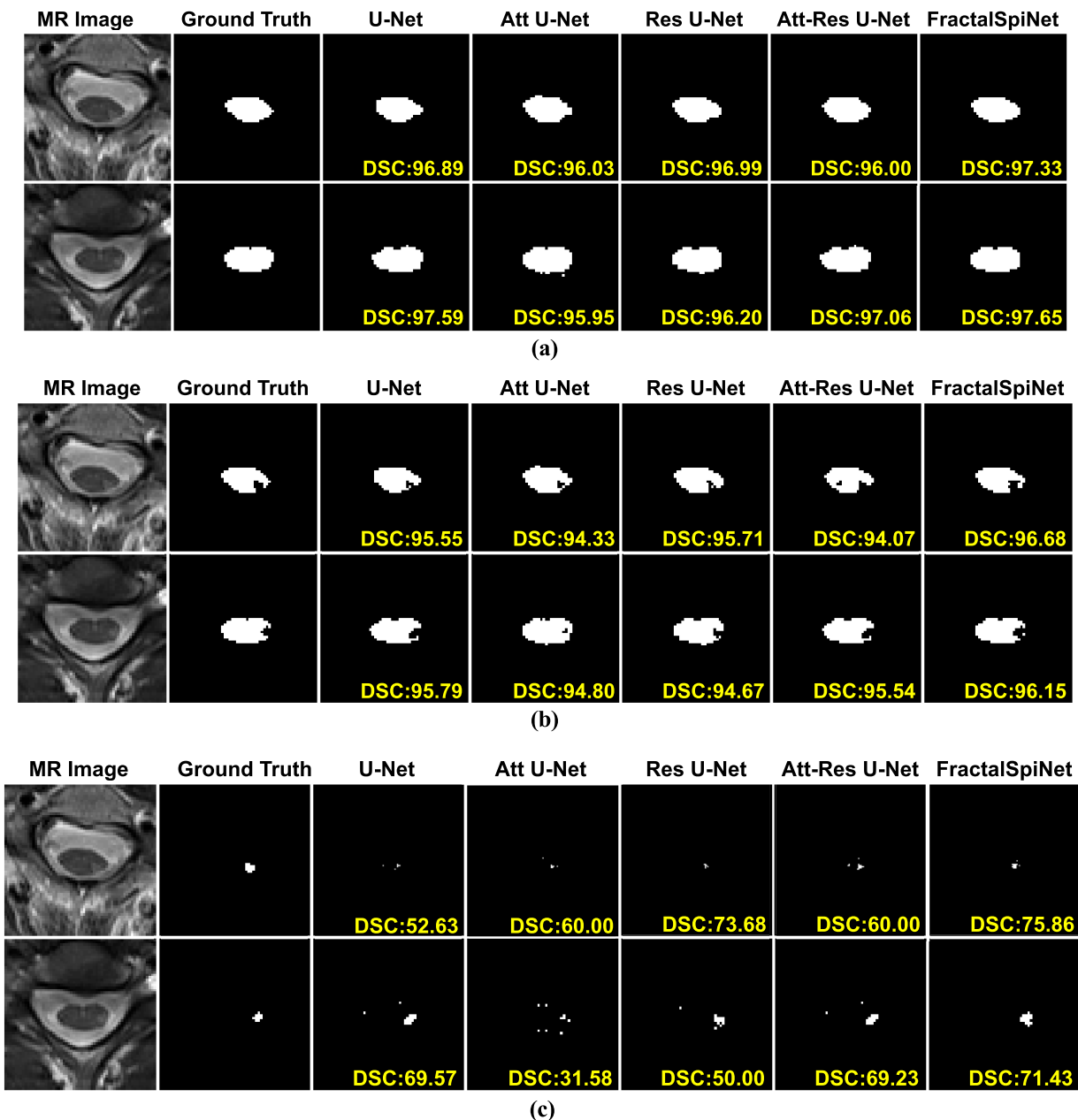
FIGURE 13. Lower successful results for the proposed FractalSpiNet architecture and other state-of-the-art models for (a) full CSA segmentation of the whole spinal cord area, (b) CSA segmentation in the spinal cord area without MS lesions, (c) segmentation of MS lesions in CSA region of cervical spinal cord.

Fig. 14 shows the visual results obtained by the methods in segmenting the CSA region and the grey matter in this region after 200 epochs of training with the same network parameters for some images in the test set of this dataset. From the results obtained for the MR images in the dataset, it can be seen that the performance of the proposed FractalSpiNet and typical U-Net models are fairly similar to each other. The other state-of-the-art methods, Att U-Net, Res U-Net and Att-Res U-Net, achieved lower performance in CSA and grey matter segmentation compared to these two models.

The performance evaluation of the results obtained using the proposed FractalSpiNet, U-Net, Att U-Net, Res U-Net and Att-Res U-Net architectures for grey matter segmentation on the Spinal Cord Grey Matter Segmentation Challenge dataset with key metrics is given in Table 7. From the results, it can be concluded that the results of the proposed Fractal-SpiNet and U-Net models are quite close and more successful than the other models. While the performance achievement in grey matter segmentation with the proposed FractalSpiNet architecture is 83.05% with the DSC metric, this ratio is
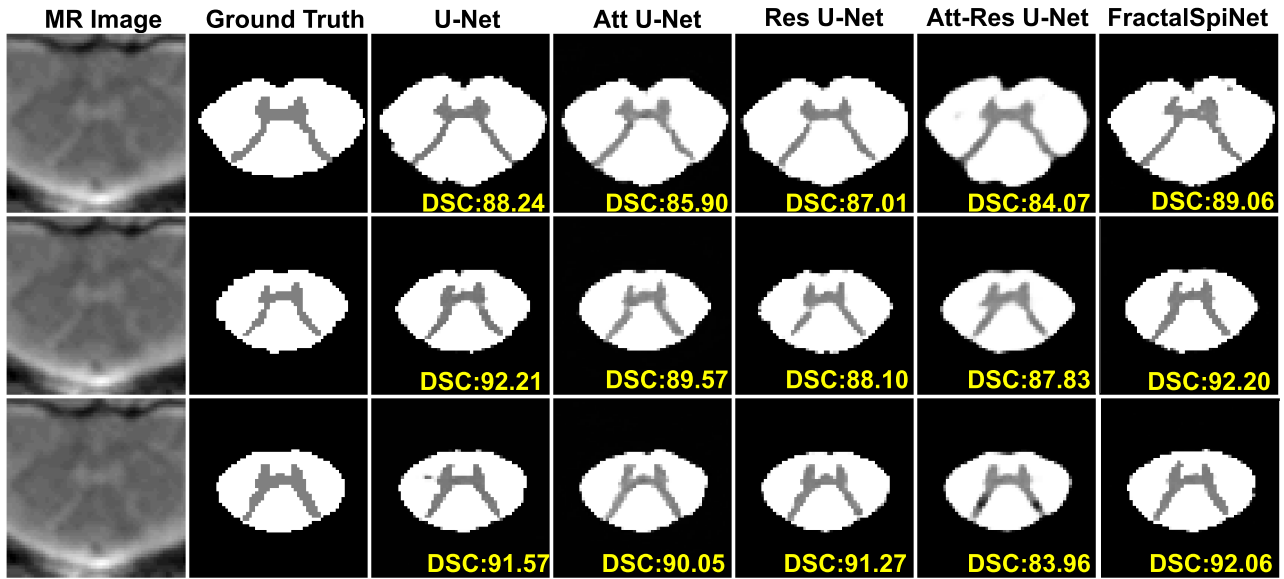
FIGURE 14. CSA and grey matter segmentation results of the proposed FractalSpiNet and other state-of-the-art methods for the Spinal Cord Grey Matter Segmentation Challenge publicly available database.

TABLE 6. Segmentation of Spinal Cord CSA Region Without MS Lesion and Key Metric Based Performance Comparisons For Proposed FractalSpiNet Architecture and Other State-of-the-art Methods.

	METHODS				
KEY METRIC	U-Net	Att U-Net	Res U-Net	Att-Res U-Net	FractalSpiNet
DSC (%)	96.18	94.42	96.64	94.50	97.17
VOE (%)	6.75	9.94	6.00	9.77	5.00
HD95 [mm]	3.03	5.01	2.90	4.93	2.45
ASD [mm]	4.89	13.13	4.34	8.32	3.72
RVD (%)	3.66	7.87	3.20	4.57	2.64
REC (%)	97.11	97.75	96.72	95.46	97.27
PRE (%)	95.43	91.58	96.75	93.79	97.20

83.20% for U-Net. The results of these two models are also very close for other metrics.

Although there are some publicly available datasets for segmentation of the spinal cord, there is no publicly available dataset that specifically includes the cervical spinal cord region and MS lesions in this region. Therefore, it is very difficult to compare the results of this study with other state-of-the-art approaches on many parameters. In addition, the different methods used in the studies make this comparison even more difficult. In addition, the key performance metrics evaluated in many studies is also different. Nevertheless, in this context, the comparison of the results obtained in this study with some state-of-the-art studies that have been

proposed previously and are similar in content to this study is shown in Table 8. Considering the difficulties of working in the cervical spine region, it can be seen that the FractalSpiNet architecture proposed in this study achieves very successful performance results. Of course, this is not a one-to-one comparison, but it can only give an idea of the method used and the DSC score obtained. Most of the previously proposed spinal segmentation studies have used the original dataset, including this study. However, Bedard et al. [63] used the spine generic public dataset, which is a publicly available dataset. On the other hand, the most recent studies mostly performed spinal cord segmentation, and there are few studies on MS lesion detection in the spinal cord. Among these studies, only Gros et al. [31] and Zhuo et al. [36] studied the detection of MS lesions in the spinal cord. In this study, using the proposed FractalSpiNet architecture on the original dataset, CSA segmentation in the spinal cord was achieved with a DSC score of 98.88%, CSA segmentation without MS lesions with a DSC score of 97.17%, and MS lesion detection in the CSA region of the cervical spinal cord with a DSC score of 90.90%, which are consistent with or higher than the results of state-of-the-art methods.

Table 9 shows the total time required by the proposed FractalSpiNet and other state-of-the-art models to detect MS lesions in the cervical spinal cord for a total of 216 MR images in the test set and the average detection time required for a single MR image. Although the detection times for the test set are close for all models, the minimum detection time for the proposed FractalSpiNet architecture is 44.42 seconds. On the other hand, the average detection time for a single MR image is approximately 0.2 seconds for all models and there is no significant difference between the models. However, the

TABLE 7. The performance evaluation of the results For FractalSpiNet, U-Net, Att U-Net, Res U-Net and Att-Res U-Net architectures for grey matter segmentation on the Spinal Cord Grey Matter Segmentation Challenge dataset.

KEY METRIC	METHODS				
	U-Net	Att U-Net	Res U-Net	Att-Res U-Net	FractalSpiNet
DSC (%)	83.20	80.40	79.24	74.79	83.05
VOE (%)	28.42	32.36	33.87	39.65	28.68
HD95 [mm]	1.33	1.55	1.72	4.25	1.39
ASD [mm]	4.84	5.83	5.59	10.78	4.84
RVD (%)	9.09	8.92	10.14	14.41	10.55
REC (%)	85.49	79.38	76.61	78.11	86.28
PRE (%)	81.35	81.98	82.65	72.47	80.42

TABLE 8. Comparison of The State-of-the-Art Studies with FractalSpiNet.

Study	Dataset	Method	DSC (%)
De Leener *et al.* (2014) [63]	Original Dataset	PropSeg	90.0 *(spinal cord segmentation)*
De Leener *et al.* (2015) [64]	Original Dataset	PropSeg	91.0 ± 0.02 *(segmentation of spinal cord and spinal canal)*
Prados *et al.* (2016) [61]	Original Dataset	OPAL algorithm and STEPS segmentation process	96.5 *(CSA segmentation with visible lesions)* 97.0 *(CSA without visible lesions)*
Gros *et al.* (2019) [24]	Original Dataset	CNN (DeepSeg)	95.9 *(spinal cord segmentation)* 60.4 *(MS lesion detection)*
Lemay *et al.* (2021) [34]	Original Dataset	Cascaded architecture with U-Net-based models	76.7 ± 1.5 *(Tumor + Cavity + Edema)*
Zhang *et al.* (2021) [32]	Original Dataset	U-Net	87.0 ± 18.4 *(CSA segmentation)*
Zhang *et al.* (2022) [37]	Original Dataset	Channel attentive U-Net (SeUneter)	90.67 ± 1.63 *(cervical spine segmentation)*
Zhuo *et al.* (2022) [35]	Original Dataset	MultiResUNet	50.0 *(MS)* 58.0 *(neuromyelitis optica spectrum disorders)*
Bedard *et al.* (2023) [62]	Spine generic public dataset	U-Net based soft segmentations	96.0 ± 1 *(spinal cord segmentetaion)*
Our study	Original Dataset	FractalSpiNet	98.88 *(CSA segmentation in spinal cord)* 97.17 *(CSA segmentation without MS lesions)* 90.90 *(MS lesion detection)*

total detection time calculated for the test set and the detection time obtained for a single MR image make it meaningful to realise real-time applications of the proposed work.

TABLE 9. Total Detection Time For Test Set And Average Detection Time For A Single Image For Models.

Method	Total detection time for test set (s)	Average detection time for a single image (s)
U-Net	45.51	0.211
Att U-Net	44.82	0.208
Res U-Net	45.17	0.209
Att-Res U-Net	44.67	0.207
FractalSpiNet	44.42	0.205

The experimental results clearly demonstrate the effectiveness of the proposed FractalSpiNet architecture over traditional U-Net models for cervical cord segmentation and MS lesion detection. However, the FractalSpiNet architecture proposed in this study has some limitations. One significant limitation of this study is the lack of publicly available datasets specifically targeting the cervical spinal cord and MS lesions. The dataset used in this study was privately created, which might limit the generalizability of the results. Public datasets would enable more robust comparisons and validation across different studies. On the other hand, the dataset consisted of MR images from 87 patients. Although the FractalSpiNet architecture performed well, a larger dataset could provide more comprehensive validation and potentially improve the model's robustness. Another limitation of the study is that some segmentation errors were observed in cases where the boundaries of MS lesions were not clearly defined. This can result in small-scale overflow or incomplete segmentation, highlighting a limitation in handling ambiguous regions in MR images.

VI. CONCLUSION

The spinal cord does not have a specific geometric shape in terms of its structure, but has a curved structure corresponding to the vertebral structure. Therefore, segmenting the region and determining its boundaries is a very challenging task. The fact that the spinal cord boundaries have a variable shape along the spinal cord and that the lesions to be detected in the spinal cord are heterogeneous in terms of location, size and shape is an important detail that needs to be considered for segmentation, although it is positive in terms of data diversity. In this study, automatic segmentation of the cervical spinal cord and detection of MS lesions in the spinal cord from MR images is achieved by using the proposed FractalSpiNet model as a fractal convolution-based hybrid U-Net architecture. In the experimental studies, using the proposed FractalSpiNet architecture, the cervical spinal cord CSA region was segmented with a DSC score of 98.88%, while MS lesions in the cervical spinal cord region were successfully detected with a DSC score of 90.90%. In addition, the cervical spinal cord (CSA) region without MS lesions was successfully segmented with a DSC score of 97.17%. In summary, the experimental results demonstrate the effectiveness of our approach in achieving accurate segmentation of the cervical spinal cord and MS lesions, surpassing state-of-the-art methods. In the most general sense, the proposed

FractalSpiNet architecture achieves higher performance than the basic U-Net model, and it is predicted that this method can be improved for future new architectures.

The ability to accurately segment the cervical spinal cord and detect MS lesions from MR images has profound implications for patient care. Early and precise identification of MS lesions is crucial for timely intervention, potentially slowing disease progression and improving patient outcomes. The FractalSpiNet model can enhance the accuracy and efficiency of radiologists, reducing the time needed for manual segmentation and increasing diagnostic confidence. This can lead to more personalized and effective treatment plans, improving the quality of life for patients with multiple sclerosis and other spinal cord-related conditions.

In MR imaging, it is not yet possible to focus on the area of interest, and there is a lot of unnecessary space in the overall MR data. For this reason, the axial plane MR image of the spinal cord corresponds to a very small area in terms of the area it covers, and MS lesions within these boundaries correspond to much smaller pixel values. Masking such small areas is very difficult, even for experienced specialists, and the possibility of error remains. In this context, segmentation of the spinal cord, different units within the spinal cord, and MS lesions in the spinal cord region with deep learning architectures is very limited due to the difficulties in preparing the dataset. In addition, the similarity of lesion densities to grey matter densities and some other textural structures are other factors that increase the possibility of error in manual masking processes. Failure to perform masking correctly will ultimately lead to training failure and subsequent detection of spinal cord and MS lesions with lower performance. In this study, a new dataset was created using MR slices of the cervical spinal cord scanned from the axial angle. For this dataset, the spinal cord region and the ground truth mask data for MS lesions were created with the consensus of two experienced radiologists. The MR images in the dataset were only scanned from the cervical region of the spinal cord, and for further studies, it is intended to segment the MS lesion along the entire spinal cord by scanning images from the thoracic and lumbar regions of the spinal cord.

ACKNOWLEDGMENT

REFERENCES

[1] N. Masse-Gignac, S. Flórez-Jiménez, J. Mac-Thiong, and L. Duong, "Attention-gated U-Net networks for simultaneous axial/sagittal planes segmentation of injured spinal cords," *J. Appl. Clin. Med. Phys.*, vol. 24, no. 10, Oct. 2023, Art. no. e14123.

[2] J. T. Kaiser, V. Reddy, M. V. Launico, and J. G. Lugo-Pico, "Anatomy, head and neck, cervical vertebrae," in *StatPearls*. Treasure Island, FL, USA: StatPearls Publishing, 2023.

[3] M. E. Atkinson, "The central nervous system," in *Anatomy for Dental Students*. Petersburg, FL, USA: StatPearls Publishing, 2013.

[4] M. Amanat, A. R. Vaccaro, M. Salehi, and V. Rahimi-Movaghar, "Neurological conditions associated with spinal cord injury," *Informat. Med. Unlocked*, vol. 16, Sep. 2019, Art. no. 100245.

[5] N. Grigoriadis and V. van Pesch, "A basic overview of multiple sclerosis immunopathology," *Eur. J. Neurol.*, vol. 22, no. S2, pp. 3–13, Oct. 2015.

[6] D. Mortazavi, A. Z. Kouzani, and H. Soltanian-Zadeh, "Segmentation of multiple sclerosis lesions in MR images: A review," *Neuroradiology*, vol. 54, no. 4, pp. 299–320, Apr. 2012.

[7] M. Pugliatti, S. Sotgiu, and G. Rosati, "The worldwide prevalence of multiple sclerosis," *Clin. Neurol. Neurosurgery*, vol. 104, no. 3, pp. 182–191, Jul. 2002.

[8] A. Nouri, L. Tetreault, A. Singh, S. K. Karadimas, and M. G. J. S. Fehlings, "Degenerative cervical myelopathy: Epidemiology, genetics, and pathogenesis," *Spine*, vol. 40, no. 12, pp. E675–E693, 2015.

[9] J. C. J. Bot, F. Barkhof, C. H. Polman, G. J. L. A. Nijeholt, V. de Groot, E. Bergers, H. J. Ader, and J. A. Castelijns, "Spinal cord abnormalities in recently diagnosed MS patients: Added value of spinal MRI examination," *Neurology*, vol. 62, no. 2, pp. 226–233, Jan. 2004.

[10] M. Patek, M. J. A. Stewart, and I. C. Medicine, "Spinal cord injury," *Lancet*, vol. 359, no. 9304, pp. 417–425, 2023.

[11] P. W. Stroman et al., "The current state-of-the-art of spinal cord imaging: Methods," *NeuroImage*, vol. 84, pp. 1070–1081, Jan. 2014.

[12] B. De Leener, M. Taso, J. Cohen-Adad, and V. Callot, "Segmentation of the human spinal cord," *Magnetic Resonance Materials Physics, Biology Medicine*, vol. 29, no. 2, pp. 125–153, 2016.

[13] M. Moccia, S. Ruggieri, A. Ianniello, A. Toosy, C. Pozzilli, and O. Ciccarelli, "Advances in spinal cord imaging in multiple sclerosis," *Therapeutic Adv. Neurological Disorders*, vol. 12, Jan. 2019, Art. no. 175628641984059.

[14] K. Weier, J. Mazraeh, Y. Naegelin, A. Thoeni, J. G. Hirsch, T. Fabbro, N. Bruni, H. Duyar, K. Bendfeldt, E.-W. Radue, L. Kappos, and A. Gass, "Biplanar MRI for the assessment of the spinal cord in multiple sclerosis," *Multiple Sclerosis J.*, vol. 18, no. 11, pp. 1560–1569, Nov. 2012.

[15] M. Filippi, P. Preziosa, B. L. Banwell, F. Barkhof, O. Ciccarelli, N. De Stefano, J. J. Geurts, F. Paul, D. S. Reich, and A. T. Toosy, "Assessment of lesions on magnetic resonance imaging in multiple sclerosis: Practical guidelines," *Brain*, vol. 142, no. 7, pp. 1858–1875, 2019.

[16] H. J. Kim, F. Paul, M. A. Lana-Peixoto, S. Tenembaum, N. Asgari, J. Palace, E. C. Klawiter, D. K. Sato, J. de Seze, and J. Wuerfel, "MRI characteristics of neuromyelitis optica spectrum disorder: An international update," *Neurology*, vol. 84, no. 11, pp. 1165–1173, 2015.

[17] R. Polattimur, E. Dandıl, M. S. Yıldırım, A. U. Senol, Z. E. Tezel, A. O. Selvi, and S. C. Kabay, "Fully automated axial plane segmentation of cervical spinal cord using U-Net in MR scans," in *Proc. 7th Int. Symp. Innov. Approaches Smart Technol. (ISAS)*, Nov. 2023, pp. 1–7.

[18] S. Mirafzal, A. Goujon, R. Deschamps, K. Zuber, J. C. Sadik, O. Gout, A. Lecler, and J. Savatovsky, "3D PSIR MRI at 3 Tesla improves detection of spinal cord lesions in multiple sclerosis," *J. Neurol.*, vol. 267, no. 2, pp. 406–414, Feb. 2020.

[19] V. S. Fonov, A. Le Troter, M. Taso, B. De Leener, G. Lévuque, M. Benhamou, M. Sdika, H. Benali, P.-F. Pradat, D. L. Collins, V. Callot, and J. Cohen-Adad, "Framework for integrated MRI average of the spinal cord white and gray matter: The MNI–Poly–AMU template," *NeuroImage*, vol. 102, pp. 817–827, Nov. 2014.

[20] M.-M. El Mendili, R. Chen, B. Tiret, N. Villard, S. Trunet, M. Pélégrini-Issac, S. Lehéricy, P.-F. Pradat, and H. Benali, "Fast and accurate semi-automated segmentation method of spinal cord MR images at 3T applied to the construction of a cervical spinal cord template," *PLoS One*, vol. 10, no. 3, Mar. 2015, Art. no. e0122224.

[21] J. Koh, T. Kim, V. Chaudhary, and G. Dhillon, "Automatic segmentation of the spinal cord and the dural sac in lumbar MR images using gradient vector flow field," in *Proc. Annu. Int. Conf. IEEE Eng. Med. Biol.*, Aug. 2010, pp. 3117–3120.

[22] J. Koh, P. D. Scott, V. Chaudhary, and G. Dhillon, "An automatic segmentation method of the spinal canal from clinical MR images based on an attention model and an active contour model," in *Proc. IEEE Int. Symp. Biomed. Imaging, From Nano Macro*, Mar. 2011, pp. 1467–1471.

[23] M. Chen, A. Carass, J. Oh, G. Nair, D. L. Pham, D. S. Reich, and J. L. Prince, "Automatic magnetic resonance spinal cord segmentation with topology constraints for variable fields of view," *NeuroImage*, vol. 83, pp. 1051–1062, Dec. 2013.

[24] C. Gros, B. De Leener, S. M. Dupont, A. R. Martin, M. G. Fehlings, R. Bakshi, S. Tummala, V. Auclair, D. G. McLaren, V. Callot, J. Cohen-Adad, and M. Sdika, "Automatic spinal cord localization, robust to MRI contrasts using global curve optimization," *Med. Image Anal.*, vol. 44, pp. 215–227, Feb. 2018.

[25] S. Pezold, K. Fundana, M. Amann, M. Andelova, A. Pfister, T. Sprenger, and P. C. Cattin, "Automatic segmentation of the spinal cord using continuous max flow with cross-sectional similarity prior and tubularity features," in *Recent Advances in Computational Methods and Clinical Applications for Spine Imaging*. Cham, Switzerland: Springer, 2015, pp. 107–118.

[26] SK. H. Ahammad, V. Rajesh, and M. Z. U. Rahman, "Fast and accurate feature extraction-based segmentation framework for spinal cord injury severity classification," *IEEE Access*, vol. 7, pp. 46092–46103, 2019.

[27] Y. Zhang, J. Wu, W. Chen, Y. Liu, J. Lyu, H. Shi, Y. Chen, E. X. Wu, and X. Tang, "Fully automatic white matter hyperintensity segmentation using U-Net and skip connection," in *Proc. 41st Annu. Int. Conf. IEEE Eng. Med. Biol. Soc. (EMBC)*, Jul. 2019, pp. 974–977.

[28] Z. Merali, J. Z. Wang, J. H. Badhiwala, C. D. Witiw, J. R. Wilson, and M. G. Fehlings, "A deep learning model for detection of cervical spinal cord compression in MRI scans," *Sci. Rep.*, vol. 11, no. 1, p. 10473, May 2021.

[29] Z. Han, B. Wei, A. Mercado, S. Leung, and S. Li, "Spine-GAN: Semantic segmentation of multiple spinal structures," *Med. Image Anal.*, vol. 50, pp. 23–35, Dec. 2018.

[30] D. W. Cadotte, A. Cadotte, J. Cohen-Adad, D. Fleet, M. Livne, J. R. Wilson, D. Mikulis, N. Nugaeva, and M. G. Fehlings, "Characterizing the location of spinal and vertebral levels in the human cervical spinal cord," *Amer. J. Neuroradiology*, vol. 36, no. 4, pp. 803–810, Apr. 2015.

[31] C. Gros, B. De Leener, A. Badji, J. Maranzano, D. Eden, S. M. Dupont, J. Talbott, R. Zhuoqiong, Y. Liu, and T. J. N. Granberg, "Automatic segmentation of the spinal cord and intramedullary multiple sclerosis lesions with convolutional neural networks," *Neuroimage*, vol. 184, pp. 901–915, Sep. 2019.

[32] D. B. McCoy, S. M. Dupont, C. Gros, J. Cohen-Adad, R. J. Huie, A. Ferguson, X. Duong-Fernandez, L. H. Thomas, V. Singh, J. Narvid, L. Pascual, N. Kyritsis, M. S. Beattie, J. C. Bresnahan, S. Dhall, W. Whetstone, and J. F. Talbott, "Convolutional neural network–based automated segmentation of the spinal cord and contusion injury: Deep learning biomarker correlates of motor impairment in acute spinal cord injury," *Amer. J. Neuroradiology*, vol. 40, no. 4, pp. 737–744, Mar. 2019.

[33] X. Zhang, Y. Li, Y. Liu, S.-X. Tang, X. Liu, K. Punithakumar, and D. Shi, "Automatic spinal cord segmentation from axial-view MRI slices using CNN with grayscale regularized active contour propagation," *Comput. Biol. Med.*, vol. 132, May 2021, Art. no. 104345.

[34] M. AskariHemmat, S. Honari, L. Rouhier, C. S. Perone, J. Cohen-Adad, Y. Savaria, and J.-P. David, "U-net fixed-point quantization for medical image segmentation," in *Large-Scale Annotation of Biomedical Data and Expert Label Synthesis and Hardware Aware Learning for Medical Imaging and Computer Assisted Intervention*. Cham, Switzerland: Springer, 2019, pp. 115–124.

[35] A. Lemay, C. Gros, Z. Zhuo, J. Zhang, Y. Duan, J. Cohen-Adad, and Y. Liu, "Automatic multiclass intramedullary spinal cord tumor segmentation on MRI with deep learning," *NeuroImage, Clin.*, vol. 31, Jul. 2021, Art. no. 102766.

[36] Z. Zhuo et al., "Automated classification of intramedullary spinal cord tumors and inflammatory demyelinating lesions using deep learning," *Radiol., Artif. Intell.*, vol. 4, no. 6, Nov. 2022, Art. no. e210292.

[37] G. Hille, J. Steffen, M. Dunnwald, M. Becker, S. Saalfeld, and K. Tonnies, "Spinal metastases segmentation in MR imaging using deep convolutional neural networks," 2020, *arXiv:2001.05834*.

[38] X. Zhang, Y. Yang, Y.-W. Shen, P. Li, Y. Zhong, J. Zhou, K.-R. Zhang, C.-Y. Shen, Y. Li, M.-F. Zhang, L.-H. Pan, L.-T. Ma, and H. Liu, "SeUneter: Channel attentive U-Net for instance segmentation of the cervical spine MRI medical image," *Frontiers Physiol.*, vol. 13, Dec. 2022, Art. no. 1081441.

[39] C. Wheeler-Kingshott, P. W. Stroman, J. Schwab, M. Bacon, R. Bosma, J. Brooks, D. Cadotte, T. Carlstedt, O. Ciccarelli, and J. J. N. Cohen-Adad, "The current state-of-the-art of spinal cord imaging: Applications," *Neuroimage*, vol. 84, pp. 1082–1093, 2014.

[40] N. J. Holland, D. M. Schneider, R. Rapp, and R. C. Kalb, "Meeting the needs of people with primary progressive multiple sclerosis, their families, and the health-care community," *Int. J. MS Care*, vol. 13, no. 2, pp. 65–74, Jul. 2011.

[41] I. Goodfellow, Y. Bengio, and A. Courville, *Deep Learning*. Cambridge, MA, USA: MIT Press, 2016.

[42] J. Wu, Y. Zhang, K. Wang, and X. Tang, "Skip connection U-Net for white matter hyperintensities segmentation from MRI," *IEEE Access*, vol. 7, pp. 155194–155202, 2019.

[43] K. O'Shea and R. Nash, "An introduction to convolutional neural networks," 2015, *arXiv:1511.08458*.

[44] X. Hu, L. Chu, J. Pei, W. Liu, and J. Bian, "Model complexity of deep learning: A survey," *Knowl. Inf. Syst.*, vol. 63, no. 10, pp. 2585–2619, Oct. 2021.

[45] W.-K. Baek, M.-J. Lee, and H.-S. Jung, "Land cover classification from RGB and NIR satellite images using modified U-Net model," *IEEE Access*, vol. 1, pp. 1–24, 2024.

[46] O. Ronneberger, P. Fischer, and T. Brox, "U-Net: Convolutional networks for biomedical image segmentation," in *Proc. 18th Int. Conf. Med. Image Comput. Comput.-Assist. Intervent.*, vol. 9351, 2015, pp. 234–241.

[47] N. Siddique, S. Paheding, C. P. Elkin, and V. Devabhaktuni, "U-net and its variants for medical image segmentation: Theory and applications," *IEEE Access*, vol. 9, pp. 82031–82057, 2021.

[48] J. Zhang, C. Li, S. Kosov, M. Grzegorzek, K. Shirahama, T. Jiang, C. Sun, Z. Li, and H. Li, "LCU-net: A novel low-cost U-net for environmental microorganism image segmentation," *Pattern Recognit.*, vol. 115, Jul. 2021, Art. no. 107885.

[49] N. S. Punn and S. Agarwal, "Modality specific U-Net variants for biomedical image segmentation: A survey," *Artif. Intell. Rev.*, vol. 55, no. 7, pp. 5845–5889, Oct. 2022.

[50] N. Siddique, S. Paheding, C. P. Elkin, and V. Devabhaktuni, "U-net and its variants for medical image segmentation: A review of theory and applications," *IEEE Access*, vol. 9, pp. 82031–82057, 2021.

[51] N. Bjorck, C. P. Gomes, B. Selman, and K. Q. Weinberger, "Understanding batch normalization," in *Proc. Advances neural information processing systems*, vol. 31, 2018, pp. 1–20.

[52] R. Azad, E. Khodapanah Aghdam, A. Rauland, Y. Jia, A. Haddadi Avval, A. Bozorgpour, S. Karimijafarbigloo, J. Paul Cohen, E. Adeli, and D. Merhof, "Medical image segmentation review: The success of U-Net," 2022, *arXiv:2211.14830*.

[53] X. Lu, D. Clements-Croome, M. J. C. M. Viljanen, and Simulation, "Fractal geometry and architecture design: Case study review," *Chaotic Modeling Simulation*, vol. 2, pp. 311–322, Jul. 2012.

[54] B. B. Mandelbrot and M. Frame, "Fractals," *Encyclopedia Phys. Sci. Technol.*, vol. 5, pp. 579–593, Jul. 1987.

[55] Z. Bai, H. Jiang, S. Li, and Y.-D. Yao, "Liver tumor segmentation based on multi-scale candidate generation and fractal residual network," *IEEE Access*, vol. 7, pp. 82122–82133, 2019.

[56] G. Larsson, M. Maire, and G. Shakhnarovich, "Fractalnet: Ultra-deep neural networks without residuals," 2016, *arXiv:1605.07648*.

[57] G. F. Roberto, A. Lumini, L. A. Neves, and M. Z. do Nascimento, "Fractal neural network: A new ensemble of fractal geometry and convolutional neural networks for the classification of histology images," *Expert Syst. Appl.*, vol. 166, Aug. 2021, Art. no. 114103.

[58] O. Oktay, J. Schlemper, L. Le Folgoc, M. Lee, M. Heinrich, K. Misawa, K. Mori, S. McDonagh, N. Y Hammerla, B. Kainz, B. Glocker, and D. Rueckert, "Attention U-net: Learning where to look for the pancreas," 2018, *arXiv:1804.03999*.

[59] Z. Zhang, Q. Liu, and Y. Wang, "Road extraction by deep residual U-Net," *IEEE Geosci. Remote Sens. Lett.*, vol. 15, no. 5, pp. 749–753, May 2018.

[60] J. Zhang, X. Lv, H. Zhang, and B. Liu, "AResU-net: Attention residual U-net for brain tumor segmentation," *Symmetry*, vol. 12, no. 5, p. 721, May 2020.

[61] R. Polattimur and E. Dandil, "12 automatic segmentation of spinal cord gray matter from MR images using a U-Net architecture," in *Explainable Artificial Intelligence for Biomedical Applications*. New York, NY, USA: River Publishers, 2023, p. 245.

[62] F. Prados, J. Ashburner, C. Blaiotta, T. Brosch, J. Carballido-Gamio, M. J. Cardoso, B. N. Conrad, E. Datta, G. David, and B. J. N. De Leener, "Spinal cord grey matter segmentation challenge," *Neuroimage*, vol. 152, pp. 312–329, Jul. 2017.

[63] S. Bédard, E. N. Karthik, C. Tsagkas, E. Pravata, C. Granziera, A. Smith, K. A. Weber, and J. Cohen-Adad, "Towards contrast-agnostic soft segmentation of the spinal cord," 2023, *arXiv:2310.15402*.
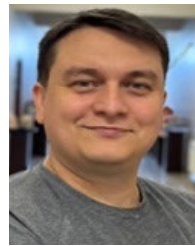
[64] B. De Leener, S. Kadoury, and J. Cohen-Adad, "Robust, accurate and fast automatic segmentation of the spinal cord," *NeuroImage*, vol. 98, pp. 528–536, Sep. 2014.

[65] B. De Leener, J. Cohen-Adad, and S. Kadoury, "Automatic segmentation of the spinal cord and spinal canal coupled with vertebral labeling," *IEEE Trans. Med. Imag.*, vol. 34, no. 8, pp. 1705–1718, Aug. 2015.
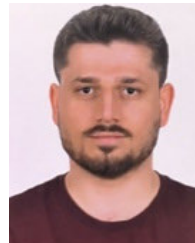
MEHMET SÜLEYMAN YILDIRIM was born in 1983. He is currently an Assistant Professor with Bilecik Şeyh Edebali University. His research interests include deep learning, medical image processing, and web-based decision support systems.

RUKİYE POLATTİMUR was born in 1989. She is currently pursuing the Ph.D. degree with the Department of Electronics and Computer Engineering, Institute of Graduate, Bilecik Şeyh Edebali University. She is a Lecturer with Bilecik Şeyh Edebali University. Her research interests include deep learning, image processing, and computer vision.

SÜLEYMAN ULUÇAY received the bachelor's degree from the Medical Faculty, in 2019, and the General Practitioner Doctor degree from Akdeniz University, Türkiye. He joined as an Assistant Doctor with Akdeniz University Hospital, in 2010, where he is currently an Assistant Doctor with the Department of Radiology. His research interests include neuroimaging, neuroradiology, and demyelinating diseases.

EMRE DANDIL received the degree in electronic and computer sciences, in 2007, the M.Sc. degree from Süleyman Demirel University, Türkiye, and the Ph.D. degree in computer engineering from Sakarya University, Türkiye, in 2015. He joined as a Lecturer with Bilecik Şeyh Edebali University, in 2010, having previously taught at the Ministry of Education for three years. He is currently an Associate Professor with the Department of Computer Engineering, Bilecik Şeyh Edebali University. He also visited the Center for Secure Information Technologies (CSIT), Institute of Electronics, Communication and Information Technology (ECIT), Queen's University Belfast, U.K., to research postdoctoral study, as a Visiting Researcher, from 2016 to 2017. He has studied there in a project relating to fetal movement detection on US scans. His research interests include artificial intelligence, image processing, pattern recognition, biomedical, machine learning, computer-aided detection, medical informatics, data mining, and computer vision.

UTKU ŞENOL received the Ph.D. degree in medical informatics. He completed his radiology residency with Akdeniz University School of Medicine, in 1993. His Ph.D. thesis was on evidence-based medicine, appropriateness imaging, and decision support systems. His thesis was on interventional radiology. In 1997, he was a Faculty Member of Akdeniz University School of Medicine, where he is currently a full-time Professor and the Head of the Neuroradiology Department. He also teaches at the Medical Informatics Program, Akdeniz University. His main focus is on functional MRI-related projects. Some of his primary competencies include MRI, imaging physics, fMRI, advanced imaging techniques, neuroradiology, and pediatric neuroradiology. He has been involved in many psychological research studies. Furthermore, it is pertinent to note that he instructs and collaborates in the management of head and neck pathologies. His research interests include imaging brain tumors, demyelinating disease, neurodegenerative disease, congenital brain malformations, stroke, full face and arm transplants, and epilepsy.

● ● ●